
Article:
Slavenko, A. orcid.org/0000-0002-3265-7715, Tamar, K., Tallowin, O.J.S. et al. (4 more authors) (2020) Cryptic diversity and non-adaptive radiation of montane New Guinea skinks (Papuascincus; Scincidae). Molecular Phylogenetics and Evolution, 146. 106749. ISSN 1055-7903

https://doi.org/10.1016/j.ympev.2020.106749

Cryptic diversity and non-adaptive radiation of montane New Guinea skinks (*Papuascincus*; Scincidae)

Alex Slavenko[1,*], Karin Tamar[2], Oliver J.S. Tallowin[3], Allen Allison[4], Fred Kraus[5], Salvador Carranza[2], Shai Meiri[1,6]

1 – School of Zoology, Tel Aviv University, 6997801, Tel Aviv, Israel
2 – Institute of Evolutionary Biology (CSIC-Universitat Pompeu Fabra), Barcelona, Spain
3 – UN Environment World Conservation Monitoring Centre, Cambridge, UK
4 – Bernice P. Bishop Museum, Honolulu, USA
5 – Department of Ecology and Evolutionary Biology, University of Michigan, Michigan, USA
6 – The Steinhardt Museum of Natural History, Tel Aviv, Israel

* – Corresponding author; slavenko@mail.tau.ac.il

ABSTRACT

New Guinea, the world's largest and highest tropical island, has a rich but poorly known biota. *Papuascincus* is a genus of skinks endemic to New Guinea's mountain regions, comprising two wide-ranging species and two species known only from their type series. The phylogeny of the genus has never been examined and the relationships among its species – as well as between it and closely related taxa – are hitherto unknown. We performed the first large-scale molecular-phylogenetic study of *Papuascincus*, including sampling across the genus' range in Papua New Guinea. We sequenced three mitochondrial and two nuclear markers from 65 specimens of *Papuascincus* and reconstructed their phylogenetic relationships. We also performed species-delimitation analyses, estimated divergence times and ancestral biogeography, and examined body-size evolution within the genus. *Papuascincus* was strongly supported as monophyletic. It began radiating during the mid-Miocene in the area now comprising the Central Cordillera of New Guinea, then dispersed eastward colonising the Papuan Peninsula. We found evidence of extensive cryptic diversity within the genus, with between nine and 20 supported genetic lineages. These were estimated using three methods of species delimitation and predominantly occur in allopatry. Distribution and body-size divergence patterns indicated that character displacement in size took place during the evolutionary history of *Papuascincus*. We conclude that the genus requires comprehensive taxonomic revision and likely represents a species-rich lineage of montane skinks.

KEYWORDS: island diversity; molecular phylogeny; mountains; species-delimitation; tropics

HIGHLIGHTS:

- *Papuascincus* is a genus of skinks endemic to montane regions of New Guinea
- *Papuascincus* contains up to 20 previously undescribed distinct genetic lineages
- High degrees of cryptic diversity highlight the need for taxonomic revision
- Divergent body sizes of sympatric lineages are suggestive of character displacement

1. INTRODUCTION

Cryptic species are distinct taxa with discrete evolutionary trajectories that have typically been classified as a single species due to morphological similarities precluding correct identification and assignment of taxonomic status (Bickford *et al.*, 2007; Jörger & Schrödl, 2013; Pante *et al.*, 2015). Although the advent of molecular phylogenetic methods has advanced our understanding and description of cryptic diversity, several regions and taxa remain woefully understudied in this regard. This is particularly true of tropical rainforest taxa (Bickford *et al.*, 2007). Tropical regions are usually among the most species-rich areas on the planet (Willig *et al.*, 2003), and many are considered as hotspots for conservation priorities (Myers *et al.*, 2000; Brooks *et al.*, 2006).

New Guinea is the world's largest tropical island and is one of the most biologically diverse regions on Earth, with high levels of vertebrate species richness and endemism (Allison, 2009). The island's size, topography, geological history, and tropical climate are all factors thought to contribute to its high level of biodiversity (Allison, 2009), and much of the island's diversity patterns closely align with elevational gradients across the island's massive mountain ranges (Diamond, 1973; Allison, 1982; Tallowin *et al.*, 2017). Recent molecular phylogenetic studies have uncovered extensive cryptic diversity on New Guinea from various taxa (birds: Marki *et al.*, 2017; fishes: McGuigan *et al.*, 2000; Kadarusman *et al.*, 2012; frogs: Oliver *et al.*, 2013; Oliver *et al.*, 2017; Lepidoptera: Craft *et al.*, 2010; reptiles: Donnellan & Aplin, 1989; Rawlings & Donnellan, 2003; Metzger *et al.*, 2010; Tallowin *et al.*, 2018).

The mountains of New Guinea reach as high as 4884 m above sea level (a.s.l; the summit of Puncak Jaya in Papua Province, Indonesia) and cover a vast extent of the island, with over a third of its land area lying above 1000 m (Allison, 2009). The formation of contemporary New Guinea and its montane topography arose through the progressive northward movement of the Australian Plate and its collision with the Pacific Plate, along with extensive island-arc accretion along the plate margin (Hall, 2002; Quarles van Ufford & Cloos, 2005; Baldwin *et al.*, 2012). Despite controversy regarding the exact timing of geological events, accretion along the leading edge of Australian Craton is thought to have begun in the early Miocene (Pigram & Davies, 1987; Hall, 2002; Baldwin *et al.*, 2012), eventually giving rise to several mountain chains along the northern coast of contemporary

New Guinea. Montane uplift of the Central Cordillera that runs along the long (W-E) axis of the island is thought to have begun much more recently, likely to have arisen no earlier than the mid-Miocene (Hall, 2002; Hill & Hall, 2003; Quarles van Ufford & Cloos, 2005). The exact timing of the orogeny of the East-Papuan Composite Terrane – comprising the Papuan Peninsula in the southeast of New Guinea – is equally contentious, with estimates ranging from initiation during the Oligocene (Pigram & Davies, 1987; Quarles van Ufford & Cloos, 2005) to more recent orogeny during the mid-Miocene (Hall, 2002; Hill & Hall, 2003). Irrespective of the exact timing, the uplift of these mountain ranges has evidently influenced New Guinea's natural diversity, by promoting speciation of lowland taxa through the formation of barriers to gene flow (Georges *et al.*, 2013; Tallowin *et al.*, 2018; Tallowin *et al.*, 2019) and through generation of novel, highly dissected montane habitats for lineages to colonize (Toussaint *et al.*, 2014; Marki *et al.*, 2017; Oliver *et al.*, 2017; Tallowin *et al.*, 2018).

The genus *Papuascincus* Allison & Greer, 1986 is endemic to the montane regions of New Guinea, occurring only at elevations above 1000 m (Allison, 1982; Allison & Greer, 1986; Fig. 1). The genus is thought to be a part of a group of mostly, but not exclusively, high-elevation skinks that includes *Lipinia*, *Prasinohaema* and *Lobulia* (Greer *et al.*, 2005). Based on shared derived characteristics Greer (1974) suggested that these four genera are closely related. This result has recently been corroborated by molecular studies – albeit with the monophyly of *Lipinia* and *Prasinohaema* not supported (Rodriguez *et al.*, 2018). *Papuascincus* is unique among the montane skinks of New Guinea in its reproductive mode. Whereas montane species of *Lobulia* and *Prasinohaema* are ovoviviparous, *Papuascincus* is oviparous, laying a fixed clutch of two eggs (Allison & Greer, 1986). This is unusual for lizards inhabiting cold, montane habitats (Meiri *et al.*, 2012) and likely creates an upper barrier on their elevational distribution due to thermoregulatory limitations on egg development (Allison, 1982).

Four species are currently described in *Papuascincus*. Two – *P. stanleyanus* (Boulenger, 1897) and *P. morokanus* (Parker, 1936) – are considered widespread, whereas two (*P. buergersi* and *P. phaeodes*) are only known from their original 1932 descriptions (Vogt, 1932; Meiri *et al.*, 2018). All four species, however, are phenotypically similar in general colouration and body shape. They mainly differ from each other in body size and in their elevational distribution, but at least *P. stanleyanus* and *P. morokanus* are otherwise

ecologically and morphologically similar (Allison, 1982). The body-size variation, along with variation in some aspects of colour patterns (*e.g.,* continuous vs. fragmented dorsolateral stripes) and various scale counts across the range, points towards the existence of undescribed diversity in the genus.

In this study, we present the first large-scale genetic sampling of *Papuascincus* throughout its range in Papua New Guinea, enabling us to explore phylogeographic relationships and genetic diversity in the genus. We used a multilocus approach including both mitochondrial and nuclear DNA sequences and performed phylogenetic analyses based on concatenated datasets. Furthermore, we conducted species-delimitation analyses, biogeographical reconstructions, and estimated the divergence times and genetic diversity between and within delimited lineages. We thus provide data concerning the diversity and distribution within *Papuascincus*, its evolution, and historical biogeography in this under-studied region of the world.

2. MATERIAL AND METHODS

2.1. Genetic sampling, DNA extraction, amplification, and sequence analysis

We collected 63 tissue samples of *Papuascincus* specimens from across its range in Papua New Guinea (Fig. 2A; Table S1) and retrieved sequences from GenBank of two additional specimens (from Linkem *et al*., 2011). Two tissue samples of *Lipinia pulchra* – currently estimated as the phylogenetically closest species to *Papuascincus* (Rodriguez *et al.*, 2018) – were used as an outgroup. We used the dataset comprised of *Papuascincus* and *Lipinia* sequences to understand the genetic structure within *Papuascincus*. To obtain calibrations for the time-calibrated phylogenetic analyses, we generated another dataset adding retrieved sequences from GenBank of more-distant relatives, based on previous studies of Australian skinks: one specimen each of *Lipinia noctua*, *Lerista lineopunctulata*, *Lerista neander*, *Notoscincus ornatus*, *Scincella lateralis* and *Sphenomorphus solomonis*, and two specimens each of *Scincella assatus* and *Lipinia pulchella* (Rabosky *et al.*, 2007; Skinner *et al.*, 2011; Rodriguez *et al.*, 2018). A total of 77 specimens was used for the analyses (Table S1).

We extracted DNA from ethanol-preserved tissue samples using the Qiagen DNeasy Blood & Tissue Kits (Qiagen, Valencia, CA, USA). We sequenced a total of three

mitochondrial markers – the ribosomal 12S rRNA (*12S*), the NADH dehydrogenase subunit 2 (*ND2*) and the NADH dehydrogenase subunit 4 (*ND4*) – and two nuclear markers – RNA fingerprint protein 35 (*R35*), and the nerve growth factor *β* polypeptide (*NGFB*). Primers and PCR conditions used for the amplification and sequencing of all markers are as detailed in Linkem *et al.* (2011). Chromatographs were assembled and edited using Geneious v.11.0.5 (Biomatter Ltd). For the nuclear markers, we identified heterozygous positions and coded them according to the standard IUPAC ambiguity codes. We translated protein-coding genes into amino acids, and we detected no stop codons, suggesting that they were not pseudogenes. We aligned sequences for each marker using MAFFT v.7.3 (Katoh & Standley, 2013) with default parameters. We tested the occurrence of recombination for the two phased nuclear-gene alignments using the Pairwise Homoplasy Index (PhiTest; Bruen *et al.*, 2006) implemented in SplitsTree v.4.14.5 (Huson & Bryant, 2006), and we detected no evidence of recombination ($P > 0.6$ for the two genes).

2.2. Phylogenetic analyses

We partitioned our dataset for phylogenetic analyses with PartitionFinder v.2 (Lanfear *et al.*, 2016), using the following parameters: linked branch lengths; BEAST models; BIC model selection; "greedy schemes" search algorithm; single partition for *12S* and by codons for the protein-coding genes *ND2*, *ND4*, *R35*, and *NGFB*. For the dataset of *Papuascincus* and *Lipinia*, we performed phylogenetic analyses under Maximum Likelihood (ML) and Bayesian Inference (BI) frameworks. We analysed the complete, mitochondrial, and nuclear concatenated datasets separately with the following partitions and relevant substitution models: *12S*+*ND2*_1+*ND4*_1 (HKY+I+G), *ND2*_2+*ND4*_2 (HKY+I+G), *ND2*_3+*ND4*_3 (TRN+G), *NGFB*_1+*NGFB*_2+*NGFB*_3+*R35*_1+*R35*_2 (K80+I), *R35*_3 (HKY+I). We conducted ML analyses in RAxML v.8.1.2, as implemented in raxmlGUI v.1.5 (Silvestro & Michalak, 2012), with the GTRGAMMA model of sequence evolution and 100 random-addition replicates. We assessed nodal support with 1000 bootstrap replicates. We conducted BI analyses with MrBayes v.3.2.6 (Ronquist *et al.*, 2012). Nucleotide substitution model parameters were unlinked across partitions, and we allowed the different partitions to evolve at different rates. We performed two simultaneous parallel runs with four chains per run (three heated, one cold) for 10^7 generations, sampling every 1000 generations for the complete concatenated dataset, and for $3x10^6$ generations with a sampling frequency of every 3000

generations for the mitochondrial and nuclear concatenated datasets. We examined the standard deviation of the split frequencies between the two runs and the Potential Scale Reduction Factor (PSRF) diagnostic, and we assessed convergence by confirming that all parameters had reached stationarity and had sufficient effective sample sizes (> 200) using Tracer v.1.6 (Rambaut *et al.*, 2014). We discarded the first 25% of trees as burn-in. We considered nodes well-supported if they received ML bootstrap values ≥ 80% and posterior probability (pp) support values ≥ 0.95.

With the aim of exploring patterns of intra-specific diversity and nuclear allele sharing within *Papuascincus*, we inferred statistical parsimony networks on the two individual nuclear genes with the program TCS v.1.21 (Clement *et al.*, 2000) implemented in PopART (Leigh & Bryant, 2015) using default settings (connection limit of 95%) and including only full length sequences. To infer haplotypes, we used the on-line web tool SeqPHASE (Flot, 2010) to convert the input and output files, and we used the software PHASE v.2.1.1 (Stephens *et al.*, 2001; Stephens & Scheet, 2005) to resolve heterozygous single-nucleotide polymorphisms in the phased alignments, with a probability threshold of 0.7 for *NGFB* and 0.5 for *R35*.

We calculated inter- and intra-specific uncorrected *p*-distances of the mitochondrial (based on GMYC/bGMYC analyses) and nuclear (based on BP&P analyses) delimited *Papuascincus* lineages (see below) for each sequenced mitochondrial marker in MEGA v.7.0.14 (Kumar *et al.*, 2016).

2.3. Species-delimitation analyses

We delimited distinct lineages within *Papuascincus* using two datasets: mitochondrial and nuclear. At the first stage we evaluated mitochondrial divergence using the ML and BI functions of the Generalized Mixed Yule-Coalescent analysis (GMYC and bGMYC, respectively; Pons *et al.*, 2006; Reid & Carstens, 2012) implemented in R v.3.4.2 (R Core Team, 2017). For these analyses we inferred a concatenated ultrametric mitochondrial haplotype tree using BEAST v.1.8.4 (Drummond *et al.*, 2012) with the following priors (otherwise by default): partitions and models as selected by PartitionFinder, 12S+ND2_1+ND4_1 (HKY+I+G), ND2_2+ND4_2 (HKY+I), ND2_3+ND4_3 (TRN+G); Yule process tree model; random starting tree; alpha prior uniform (0–10), strict clock prior (uniform distribution; mean 1, 0–1). We carried out three individual runs of 10^7 generations,

sampling at intervals of 1000 generations. We evaluated convergence, posterior trace plots, effective sample sizes (ESS > 200), and burn-in in Tracer v.1.6 (Rambaut *et al.*, 2014). We combined the tree runs in LogCombiner, discarded the first 10% of trees as burn-in, and generated an ultrametric tree with TreeAnnotator (both provided with the BEAST package). For the GMYC analysis we used the *splits* R package (Ezard *et al.*, 2009), applying a single threshold algorithm. For the bGMYC analysis we used the *bGMYC* R package (Reid & Carstens, 2012) to calculate marginal posterior probabilities of lineage limits from a subsample of 250 trees; we ran MCMC chains for each tree for 10^4 generations with 10% burn-in.

As a second step of species delimitation, we evaluated nuclear divergence and tested the mitochondrial GMYC/bGMYC candidate species with Bayesian Phylogenetics and Phylogeography v.3.4 (BP&P; Rannala & Yang, 2003; Yang & Rannala, 2010) using the full phased nuclear loci only. As prior distributions on the ancestral population size (θ) and root age (τ) can affect the posterior probabilities for models (Yang & Rannala, 2010; Zhang *et al.*, 2011), we performed a preliminary analysis estimating the two parameters under the MSC model with a given species phylogeny (A00 configuration, with the topology obtained using the concatenated dataset; Rannala & Yang, 2003). We parameterized these priors through Inverse Gamma distributions setting α=3 and two values of β (0.002, 0.2) that cover different alternative scenarios for ancestral population size and root age. The suggested values were (Inv-Gamma(α,β)): θ = Inv-Gamma(2, 0.2) and τ = Inv-Gamma(2, 0.01), with which we carried out two types of analyses, setting the initial number of lineages to 20 (recovered from the GMYC/bGMYC analysis, see Results): (i) A10 configuration – conducting Bayesian species delimitation analysis using a user-specified guide tree (with the topology obtained using the concatenated dataset; Yang & Rannala, 2010; Rannala & Yang, 2013), and (ii) A11 configuration – implementing a joint analysis conducting Bayesian species-delimitation while estimating the species tree (Yang & Rannala, 2014; Yang, 2015). For these analyses we used algorithms 1 and 0, assigning each species-delimitation model equal prior probability. We estimated the locus rate parameter that allows variable mutation rates among loci with a Dirichlet prior (α = 2). We set the heredity parameter that allows θ to vary among loci as default, due to our dataset being autosomal. Each rjMCMC analysis ran for $5x10^5$ generations with 10% discarded as burn-in. We considered probability values ≥ 0.95 in

all the different alternative scenarios for ancestral population size and root age as strong evidence for delimited lineages.

2.4. Estimation of divergence times and biogeographic analyses

We estimated divergence times with BEAST and the concatenated dataset containing one sample per GMYC/bGMYC-delimited lineage (see Results) and one sequence for each of the outgroups (see Table S1). We set the following divergence times, as previously estimated in other studies: (a) between the clade containing *Lerista*, *Notoscincus,* and *Sphenomorphus*, and the clade containing *Scincella*, *Papuascincus*, and *Lipinia*, to 29.4–55.8 Mya (normal distribution; mean 37 Mya, sd = 4) (Skinner *et al.*, 2011), (b) between *Scincella lateralis* and the clade containing *Papuascincus* and *Lipinia* to 20.6-43.9 Mya (normal distribution; mean 32±7 Mya) (Skinner *et al.*, 2011), (c) between *Sphenomorphus solomonis* and the clade containing *Lerista* and *Notoscincus* to 24.3-48.5 Mya (normal distribution; mean 33±4 Mya) (Skinner *et al.*, 2011), (d) between *Notoscincus ornatus* and the clade containing *Lerista* to 19.1-53.6 Mya (lognormal distribution; mean 28.2; log(sd) = 0.35, offset 5) (Rabosky *et al.*, 2007), and (e) between *Lerista lineopunctulata* and *Lerista neander* to 12.9-22.1 Mya (normal distribution; mean 17.5±2.8 Mya) (Rabosky *et al.*, 2014).

We conducted biogeographic analyses using Bayesian Stochastic Search Variable Selection (BSSVS; Lemey *et al.*, 2009) implemented in BEAST. For these analyses we used the same dataset as in the divergence-time estimates mentioned above, but for one GMYC/bGMYC lineage that was distributed in more than one discrete elevational region, we added a single specimen to represent all regions occupied by that lineage (*i.e.*, adding specimen 7662 to lineage T). We performed the biogeographic analyses twice, assigning all specimens to geological and elevational regions based on the current distribution of the genus. In one analysis we assigned the lineages to one of four discrete geological regions: (1) AC - Australian Craton; (2) FB - Fold Belt; (3) EPCT - East-Papuan Composite Terrane; and (4) OAT - Oceanic Arc Terranes. In the second analysis we assigned the lineages to one of four discrete elevational regions: (1) A – alpine (> 3000 m); (2) SA – subalpine (2500-3000 m); (3) HM - higher montane (1500-2500 m); and (4) LM – lower montane (1000-1500 m) based on the habitat categorization of Bryan & Shearman (2015).

We conducted the calibration and the two biogeographical analyses in BEAST v.1.8.4 with the following partitions and relevant models as determined by PartitionFinder:

12S+ND2_1+ND4_1 (GTR+I+G), ND2_2+ND4_2 (GTR+I+G), ND2_3+ND4_3 (TRN+G), NGFB_1+NGFB_2+NGFB_3+R35_1+R35_2 (K80+G), R35_3 (HKY+G). Other priors were as detailed above, apart from base-substitution parameter (0–100), and uncorrelated relaxed-clock model for the mitochondrial genes (uniform distribution; 0–1). For the ancestral-area reconstruction analyses additional priors were: symmetric discrete-trait substitution model, strict-clock model for the location trait, and exponential prior for the discrete-location state rate (locations.clock.rate) with mean of 1.0 and offset of 0. We conducted three individual runs of 10^8 generations for each of the three analyses, with sampling at intervals of every 10^4 generations. We evaluated convergence, posterior trace plots, effective sample sizes (ESS > 200), and burn-in with Tracer. We combined the tree runs in LogCombiner, discarding the first 10% as burn-in, and generated an ultrametric tree with TreeAnnotator.

2.5. Body-size evolution

We used the time-calibrated phylogenetic tree constructed in Section 2.4 to map adult body size onto the phylogeny. We used digital calipers to measure snout-vent-lengths (SVLs) to the nearest 0.1 mm of 533 adult specimens representing the various lineages, including 62 specimens vouchered with tissues (Table S2). We assigned the specimens that were not sampled genetically to the different delimited lineages based on sampling localities and dates and general morphological similarity in colour patterns and size. Thus, specimens that were collected from the same population, and during the same collecting expedition as voucher specimens that were sampled genetically, were assigned to the same lineage of similar-sized genetic vouchers with a similar colour pattern. We excluded juveniles and subadults – as determined based on dissection and visual examination of gonads – from this analysis. We then calculated the mean SVL for each GMYC/bGMYC and BP&P-delimited lineage. We mapped the mean SVL onto the tips of the time-calibrated phylogeny and used the *fancyTree* and *phenogram* functions in the *phytools* package (Revell, 2012), implemented in R v.3.4.2 (R Core Team, 2017), to visualize body-size evolution along the phylogeny. We compared SVLs between the different GMYC/bGMYC-delimited lineages using ANOVA with *post-hoc* Tukey tests, and we generated boxplots to visualize differences in SVL between lineages.

3. RESULTS

Our dataset comprised 65 specimens of *Papuascincus* and 12 outgroup specimens, together with a concatenated length of 3302 bp divided into three mitochondrial gene fragments (*12S*, 392 bp; *ND2*, 1020 bp; *ND4*, 708 bp) and two nuclear gene fragments (*NGFB*, 546 bp; *R35*, 636 bp).

Both the ML and BI phylogenetic trees of the complete concatenated dataset recovered the same topologies, with high support values for most nodes (Figs. 2B & S1). The topology of the phylogenetic tree based on the complete concatenated dataset is highly congruent with the topology based on the mitochondrial concatenated dataset only (Fig. S2A), although less so for the topology based on the nuclear concatenated dataset alone (Fig. S2B). We recovered *Papuascincus* as monophyletic. The GMYC and bGMYC species-delimitation analyses recovered 20 delimited mitochondrial lineages within *Papuascincus* (labelled A-T; Figs. 2B & S3). Using these 20 lineages the BP&P analyses of the nuclear data recovered only nine delimited lineages (numbered I-IX), mostly representing clustering of several GMYC/bGMYC-delimited lineages into single BP&P-delimited lineages (Fig. 2B). Only BP&P lineages V and VIII represent a single GMYC/bGMYC lineage each (L and R, respectively).

Based on the complete concatenated phylogenetic tree, the earliest split in *Papuascincus* separated the genus into two clades: (1) a "western" clade containing BP&P lineages I-III (GMYC/bGMYC lineages A-H), distributed on the Central Cordillera, the Finisterre Mts and the westernmost Owen Stanley Mts (localities 10-20 in Fig. 2A), and (2) an "eastern" clade containing BP&P lineages IV-IX (GMYC/bGMYC lineages I-T), distributed on the Central Highlands portion of the Central Cordillera and throughout the Owen Stanley Mts (localities 1-10, 13-15 and 17 in Fig. 2A).

Genetic distances among the nine BP&P-delimited lineages were greater than the genetic distances within the lineages for all three mitochondrial gene fragments (Table S3). The lowest genetic divergence among lineages in the *ND2* and *ND4* markers was found between BP&P lineages VIII and IX (*12S*: 3.2%; *ND2*: 9.4%; *ND4*: 9.7%), whereas in the *12S* marker, the distance between BP&P lineages VI and VIII was the lowest (*12S*: 3%; *ND2*: 12.8%; *ND4*: 12.5%). Similarly, genetic distances between the 20 GMYC/bGMYC-delimited lineages (Table S4) were mostly greater than the genetic distances within lineages, although

the between-lineage distances of some lineage pairs were much lower than the average between-lineage distances and even comparable to some within-lineage distances (*e.g.*, in the *12S* marker the distance between GMYC/bGMYC lineages S and T was 0.3%).

We recovered 35 unique haplotypes in the *NGFB* gene fragment and 53 unique haplotypes in the *R35* gene fragment. Of the BP&P-delimited lineages (Fig. 2C), lineages IV and V shared alleles in the *NGFB* network, lineages VII and VIII shared alleles in the *R35* network, and lineages VI and VII shared alleles in both *NGFB* and *R35* networks. No other lineages shared any alleles. More of the GMYC/bGMYC-delimited lineages shared alleles, but similarly to the BP&P lineages, few lineages shared alleles in both the *NGFB* and *R35* networks (Fig. S4).

The time-calibrated phylogenetic tree based on the dataset containing only a single representative from each GMYC/bGMYC-delimited lineage had a similar topology to the concatenated ML and BI trees (Fig. S5). We recovered the split of *Papuascincus* from its sister taxon, *Lipinia pulchra*, to have occurred roughly 14.4 Mya (95% highest posterior density [HPD]: 11.15-17.52). The sampled lineages within the genus *Papuascincus* then began radiating roughly 11.6 Mya (HPD: 9.25-14.15) in the mid-Miocene, with most of our sampled lineages arising during the late Miocene and Pliocene, between ~10 and 3 Mya. While some of the GMYC/bGMYC-delimited lineages arose during the Pleistocene, all the BP&P-delimited lineages had arisen by the end of the Pliocene.

According to the BSSVS analyses of geological ancestral reconstruction, *Papuascincus* originated with high probability on the Fold Belt (Fig. 3A). This was then followed by at least two independent colonisations of the East-Papuan Composite Terrane – once in the late Miocene by the clade giving rise to GMYC/bGMYC lineages M-T, distributed throughout the Papuan Peninsula (locations 1-9 in Fig. 2A), and a second time in the Pliocene by GMYC/bGMYC lineage E, which is restricted to Mt Missim (location 10 in Fig. 2A). There was also a single colonization event of the Oceanic Arc Terranes in the late Miocene – by GMYC/bGMYC lineage B, which is restricted to the Huon Peninsula (location 12 in Fig. 2A) – and a single colonization event of the Australian Craton in the early Pleistocene – by GMYC/bGMYC lineage G, which is restricted to Mt Bosavi (location 11 in Fig. 2A).

Our BSSVS reconstruction of *Papuascincus* according to elevational regions indicates that the ancestral population of the genus had, with a high probability, a higher montane elevational distribution (1500-2500 m in today's biome elevations – although the exact

elevations that make up the same climatic conditions might well have been different in earlier geological periods; Fig. 3B). Based on this analysis, at least three independent transitions occurred from higher montane to lower montane (1000-1500 m) elevational distributions – by GMYC/bGMYC lineages E, M and T – and at least one transition each to subalpine (2500-3000 m) and alpine (> 3000 m) elevational distributions, by lineages I and S, respectively.

Adult SVLs of *Papuascincus* varied between 36.3 mm and 67.8 mm (Table S2; Figs. 4 & S6). The subclade containing GMYC/bGMYC lineages A-H is comprised of mostly small-sized lineages, with mean SVLs of 50.8 mm or less (the "small" morph). The subclade containing GMYC/bGMYC lineages I-T was comprised of mostly large-sized lineages, with mean SVLs of 52.5 mm or higher (the "large" morph), except GMYC/bGMYC lineage L (mean SVL 48.8 mm). Almost all lineages from the "large" morph were significantly larger than almost all lineages from the "small" morph (exceptions were almost all in cases where sample sizes were exceedingly small; Table S5).

4. DISCUSSION

4.1. Cryptic diversity and evolutionary history

Our study provides the first large-scale time-calibrated phylogenetic analyses of the genus *Papuascincus*, currently endemic to montane regions in New Guinea. Our results confirm that *Papuascincus* is a valid, monophyletic genus, as previously considered based on its unique synapomorphy: pustulate surface structures on the egg shells (Allison & Greer, 1986). This corroborates previous preliminary results based on two samples each in the molecular studies of Linkem *et al.* (2011) and Rodriguez *et al.* (2018).

Using three different species-delimitation approaches based on both nuclear and mitochondrial datasets, we uncovered as little as nine and as many as 20 distinct genetic lineages, many of which may merit evaluation as separate species. Genetic divergence in mitochondrial markers between both GMYC/bGMYC and BP&P-delimited lineages was high (Tables S3 and S4), and they shared few nuclear haplotypes (Figs. 2C & S4; although shared haplotypes may be indicative of gene flow or of incomplete lineage sorting). Furthermore, our time-calibrated phylogeny revealed deep splits between BP&P-delimited lineages, mostly occurring during the late Miocene and Pliocene.

The different lineages, however, are difficult to tell apart via general morphometric proportions, colouration patterns and scalation (AS, pers. obs.) – although less so in size (Figs. 4 & S6). As far as is known, all members of *Papuascincus* have many similarities in their ecologies: they are all diurnal, insectivorous, oviparous, mostly terrestrial lizards, occurring in open habitats such as tree-fall gaps, cliff faces, forest clearings and alpine grasslands (Allison, 1982; Allison & Greer, 1986). Closely related lineages within *Papuascincus* are mostly distributed allopatrically (*e.g.*, the non-overlapping distributions of the "eastern" clade *Papuascincus* lineages in the Papuan Peninsula; Fig. 2). A lack of suitable habitat between the open habitat patches *Papuascincus* favours could appear in two forms: either as low-elevation barriers between montane regions (but see below), such as the Kokoda Gap in the Owen Stanley Mts, or continuous dense forest canopy without open habitats that precludes basking opportunities. Both would generate geographic barriers that could maintain reproductive isolation, and without divergence in ecological specialization by the different lineages, phylogenetic inertia or stabilizing selection could maintain niche conservatism and phenotypic similarity (Wiens & Graham, 2005; Losos, 2008).

4.2. Biogeographic history

The precise timing of the uplift of New Guinea's Central Cordillera is still debated. The formation of these mountains, spanning New Guinea's W-E axis, resulted from a complex geological history involving the northern movement of the Australian Plate margin and collision with the Pacific Plate, and repeated events of subduction, orogenic uplift and terrane accretion (Pigram & Davies, 1987; Hall, 2002; Baldwin *et al.*, 2012). Whereas some studies time the uplift of the Central New Guinea Highlands to have occurred in the mid-Miocene, ~12 Mya (Quarles van Ufford & Cloos, 2005), others have suggested this uplift to have begun as recently as 5 Mya (Hill & Hall, 2003) or as early as 25 Mya (Pigram & Davies, 1987). This uplift was complemented by docking of numerous accreted terranes, forming several isolated mountain ranges on New Guinea's north coast, as well as the docking of the entire East-Papuan Composite Terrane, forming the Papuan Peninsula with its Owen Stanley Mountain Range.

Our results support a relatively old, mid-Miocene origin of New Guinea's Central Cordillera, with a 11.6 Mya origin of the montane *Papuascincus* skinks on the Fold Belt (Fig. 3), congruent with previous phylogenetic studies suggesting similar dates for the orogenic

events (Toussaint *et al.*, 2014; Oliver *et al.*, 2017; Tallowin *et al.*, 2018). The uplift of the central mountain ranges likely drove the radiation of these skinks, with the likely ancestral range of the Central Cordillera occupied by 10 of the GMYC/bGMYC-delimited lineages (A, C-D, and G-L) and five of the BP&P-delimited lineages (I-V). Due to a lack of fossil data for the studied taxa, we used secondary calibrations which may give erroneous divergence time estimates (Schenk, 2016), and the true divergence times may therefore be different than estimated here.

A second radiation of *Papuascincus* then occurred ~7.5 Mya, following dispersal to the East-Papuan Composite Terrane and colonization of the Owen Stanley Mts. These mountains may have arisen during the mid-Miocene (Hill & Hall, 2003), or even earlier during the Oligocene or Eocene, followed by docking with the remainder of New Guinea during the mid-Miocene (Pigram & Davies, 1987), before possibly experiencing renewed uplift and exhumation during the Pliocene (Quarles van Ufford & Cloos, 2005).

Finally, there is GMYC/bGMYC lineage B, the sole representative of the genus on the Huon Peninsula (location 12 in Fig. 2A). The Huon Peninsula is part of the accreted Finisterre Terrane, estimated to have begun colliding with northern New Guinea during the late Miocene (Hill & Raza, 1999; Baldwin *et al.*, 2012) or Pliocene (Weiler & Coe, 2000). The dearth of high-elevation frogs in the Huon Peninsula has been suggested as evidence that the region is isolated from source areas in the Central Highlands (Zweifel, 1980). Zwiefel (1980) also suggested that the Huon Peninsula is geologically young due to low rates of endemism. Geological evidence likewise suggests the Huon Peninsula to have only been subaerially connected to New Guinea very recently, during the late Pliocene (Abbott *et al.*, 1994; Abbott, 1995; Hill & Raza, 1999). We recovered the divergence between the Huon lineage and its closest relative (within BP&P lineage I) – GMYC/bGMYC lineage A from Baiyer Gorge – to have occurred ~7.3 Mya, much earlier than the proposed subaerial connection between the Huon Peninsula and New Guinea. However, there is a pronounced gap in our sampling in the eastern Central Highlands (Fig. 1), raising the possibility that the closest lineage to the Huon Peninsula animals wasn't sampled in this study. It is likely that *Papuascincus* colonized the Huon Peninsula from the Central Highlands following the collision and uplift of the mountain ranges, bridging the low-elevation Ramu-Markham Valley between the Finisterre Mts and the Central Cordillera (Fig. 1). While this gap currently represents inhospitable habitat for *Papuascincus*, several studies have suggested

depressions of habitat boundaries in the mountains of New Guinea by hundreds of meters during glaciation periods (Hope & Golson, 1995; Porter, 2000). Data on the dispersal capabilities of *Papuascincus* are lacking, and ecological studies of them are sorely needed to fully answer this question.

4.3. Body-size evolution

Papuascincus lineages seem to differentiate based on size, with seemingly two "morphs" – small (SVL ≤ 51 mm) and large (SVL ≥ 52.5 mm). There appears to be a strong phylogenetic signal in SVL, with the "western" clade (GMYC/bGMYC lineages A-H; BP&P lineages I-III) comprised of the small morph, whereas the "eastern" clade (GMYC/bGMYC lineages I-T; BPP lineages IV-IX) is comprised mostly of the large morph, with the exception of the relatively small-sized GMYC/bGMYC lineage L from Mt Strong (BP&P lineage V; mean SVL 48.8 mm). The two size morphs also seem to differ in colour pattern (Fig. 4A), with lizards of the small morph typically having continuous dorsolateral stripes, whereas those belonging to the large morph typically have fragmented dorsolateral stripes (juveniles of the large morph, although similar in SVL to adults of the small morph, also have fragmented dorsolateral lines; A.S., pers. obs.). The differences in size between lineages from the large and small morphs were almost always significant (Table S5), with the exceptions mostly being in comparisons with lineages C, M and S, all three of which only have a single specimen each.

The spatial distribution of the two lineages may help explain the differences in body size. Whereas most lineages occur in allopatry, a few lineage pairs are sympatric: lineage C is sympatric with lineage K in Keltiga (near Mt Hagen), lineage F is sympatric with lineage J in Rondon Ridge (also near Mt Hagen), and lineage L is sympatric with lineage N on Mt Strong. In all three cases, one lineage in each pair (C, F, and L) is of the small morph, whereas the other lineage (J, K, and N) is of the large morph. Although under-sampling may result in us missing other cases of sympatry between different lineages, a more conservative interpretation using the wider-ranging BP&P lineages (II and III sympatric with IV in the vicinity of Mt Hagen; V sympatric with VI on Mt Strong) reveals the same general pattern: no two lineages of similar size occur in sympatry. The likelihood to get three cases of sympatry of different morphs by chance from a pool of 20 lineages is only 14%, lending

credence to a scenario whereby this distributional pattern was generated by a biological mechanism.

Such a spatial distribution, with no overlap in size between sympatric lineages, can arise by character displacement (Brown & Wilson, 1956; Slatkin, 1980; Dayan & Simberloff, 2005; Grant & Grant, 2006) or through species sorting (Grant, 1972; Davies *et al.,* 2007). Discerning between the two mechanisms from present distributions can be difficult, and they are not mutually exclusive. However, we offer three lines of evidence in support of character displacement. First, BP&P lineage IV is comprised of GMYC/bGMYC lineages I-K. The smallest of the three, lineage I, occurs on high elevations by Mt Hagen and seemingly not in sympatry with any other lineage. However, the two larger lineages J and K occur in sympatry with the small-sized lineages F and C, respectively, both in localities in the vicinity of Mt Hagen. Second, the smallest lineage in our sample , GMYC/bGMYC lineage E (significantly smaller than all other lineages apart from lineage C; Table S5), occurs in sympatry with a large morph on Mt Missim for which we were unable to obtain tissues for molecular analyses (A.A., pers. obs.). Third, lineage B, which occurs on the Huon Peninsula with no congeners, is the largest of the small-sized lineages, even when compared to its sister lineage A (Fig. 4), possibly suggestive of character release allowing lineage B to achieve a comparatively larger size (Simberloff *et al.*, 2000).

Several unanswered questions regarding size evolution in this group remain, with the foremost being why most of the large-sized lineages are distributed in the Papuan Peninsula, seemingly without small-sized congeners occurring in sympatry (Figs. 1 & 2)? What drove the evolution of large size particularly in this clade remains to be examined.

4.4. Taxonomic implications

There are currently four described species in the genus *Papuascincus*: *P. stanleyanus* (the type species), *P. morokanus*, *P. buergersi* and *P. phaeodes* (Allison & Greer, 1986; Uetz *et al.*, 2019). The genus was diagnosed based on a combination of derived traits, including fused frontoparietals, lower eyelid with a clear or semi-translucent window, slightly expanded basal subdigital lamellae, smooth body scales, and pustulate egg-shell surfaces (Allison & Greer, 1986) – traits which all occur in our measured specimens (apart from the poorly sampled GMYC/bGMYC lineages C, G and S, all other lineages had female specimens with oviductal eggs; A.S., pers. obs.). Our analyses, based on broad genetic sampling,

516 recovered *Papuascincus* as a monophyletic genus, congruent with preliminary results from
517 previous phylogenetic studies (Linkem *et al.*, 2011; Rodriguez *et al.*, 2018). However, our
518 phylogenetic reconstruction and estimates of divergence times and genetic distances
519 strongly suggest the existence of currently unrecognized diversity in the genus, with
520 multitudes of lineages potentially meriting recognition as different species.
521 *Papuascincus stanleyanus* (Boulenger, 1897) was originally described as *Lygosoma*
522 *stanleyanum*, based on collections made from Mt Victoria (Fig. 1) in the Owen Stanley Mts
523 by Mr A.S. Anthony (Boulenger, 1897). It is a medium-sized skink (holotype SVL = 57 mm;
524 Boulenger, 1897) that has since been reported from montane regions throughout New
525 Guinea. It has been recorded to occur in high elevations, above 1700 m, but not higher than
526 3000 m. At those elevations *P. stanleyanus* likely reaches physiological limits on egg
527 development imposed by low temperatures, and it is replaced by ovoviviparous species
528 from other genera (Allison, 1982). Based on SVL and proximity to the type locality, Mt
529 Victoria, we infer three BP&P lineages (VII, VIII and IX) as candidates to represent 'true' *P.*
530 *stanleyanus*. However, the relatively restricted distributions of these lineages suggest that *P.*
531 *stanleyanus* is distributed only in the Owen Stanley Mts, with similar-sized animals from
532 other parts of New Guinea, particularly the distantly related Central Highlands lineage IV,
533 representing yet to be described distinct species.
534 *Papuascincus morokanus* (Parker, 1936) is a smaller (SVL of the type specimens = 43-47
535 mm; Parker, 1936) skink. It was described from two specimens collected by Dr L. Loria from
536 Moroka, a locality in the eastern Owen Stanley Mts (Fig. 1). It has since been reported
537 throughout most of the lower montane regions of New Guinea (Parker, 1936; Allison &
538 Greer, 1986), ostensibly being replaced by *P. stanleyanus* above 1700 m (Allison, 1982).
539 Despite many of our sampled lineages having similar SVLs to *P. morokanus*, none of them is
540 from the vicinity of Moroka, and the type specimens of *P. morokanus* exhibit a unique
541 dorsal colour pattern that is absent from all specimens we examined (two longitudinal
542 dorsal stripes; A.S., pers. obs.). We therefore think it unlikely that we have representatives
543 of this species sampled in this study, and we suspect its true distribution is much narrower
544 than previously believed.
545 *Papuascincus buergersi* and *Papuascincus phaeodes* (Vogt, 1932) are two poorly known
546 species collected by Dr J. Bürgers during the 1912-13 Kaiserin-Augusta-Fluss expedition to
547 the Sepik River Basin. The two species were described by Vogt (1932), with no specific

548 locality data given. They are not known from any collections since (Meiri *et al.*, 2018), and
549 little is known of their biology or natural history, apart from *P. buergersi* (52-60 mm; Vogt
550 1932) having similar SVL to *P. stanleyanus*, and *P. phaeodes* (45 mm; Vogt 1932) having
551 similar SVL to *P. morokanus*. The expedition likely reached high elevations typical of
552 *Papuascincus* (Fig. 1) in the Hunstein and Schrader ranges (Sauer, 1915), making those likely
553 candidates for the *terra typica* of either species. The small-sized BP&P lineage II, from the
554 Kaironk Valley (locality 20 in Fig. 2A), is therefore a possible candidate for *P. phaeodes*, but
555 confirmation of this hypothesis will require careful comparison to type material and further
556 research into Bürgers' itinerary to identify the type localities of these two enigmatic species.
557 Animals that fit the generic description of *Papuascincus* have also been collected in the
558 Indonesian New Guinea mountains of Papua Province (A.A., pers. obs.), and are currently
559 housed in the collections of the Bernice P. Bishop Museum in Honolulu, Hawaii. They are
560 phenotypically similar in SVL and colour morph to members of the large morph (A.S., pers.
561 obs.). Unfortunately, we were unable to obtain tissue samples for molecular analyses for
562 these animals, and so we are unable to assign them to any genetic lineages.
563 Although our molecular analyses recovered between nine and 20 distinct lineages of
564 *Papuascincus*, the species-delimitation methods we used have been criticized as being
565 sensitive to incomplete geographic sampling and delimiting only genetic structure, and so to
566 be of limited use for assignment of lineages to species (*e.g.*, Olave *et al.*, 2014; Jackson *et*
567 *al.,* 2017; Sukumaran & Knowles, 2017; Hillis 2019; Leaché *et al.* 2019). We therefore avoid
568 making any taxonomic suggestions yet, as a revision of *Papuascincus*, together with
569 descriptions of new species, will require thorough morphological examination and
570 comparisons to type material, work which we are currently undertaking. However, since we
571 suspect there are no available samples for genetic analyses from the *terra typica* of at least
572 three of the four currently recognized species, focused field expeditions to the type
573 localities will be of great value in resolving the taxonomy within this endemic genus.
574
575 **4.5. Conclusions**
576 We have uncovered considerable genetic diversity in an endemic radiation of New
577 Guinean montane skinks. This further exemplifies the importance of mountains in tropical
578 regions as cradles and generators of biodiversity (Weir, 2006; Elias *et al.*, 2009; Santos *et al.*,
579 2009; Sedano & Burns, 2010; Hutter *et al.*, 2013; Chazot *et al.*, 2016), and should the

different lineages described here be elevated to species status, this would place *Papuascincus* as one of the richest lineages of lizards on the New Guinean mountains.

Despite New Guinea's lizard fauna being most diverse in lowland regions (Tallowin *et al.*, 2017), our results showcase the high-elevation habitats of the island to house unique, endemic radiations, comparable to what is found in other New Guinea taxa such as birds (Mayr & Diamond, 1976; Fritz *et al.*, 2012), amphibians (Oliver *et al.*, 2017), plants (Givnish *et al.*, 2015), and insects (Toussaint *et al.*, 2014). This emphasizes the importance of New Guinea's mountains as unique centres of biodiversity deserving particular conservation attention.

ACKNOWLEDGEMENTS

We thank Molly Hagemann (Bernice P. Bishop Museum), Lauren Scheinberg (California Academy of Sciences), Steve Donellan and Alejandro Velasco Castrillon (South Australian Museum), and Erez Maza (Steinhardt Museum of Natural History), for facilitating generous loans of tissue samples and voucher specimens used in this study. This work was supported by BSF grants no. 2012143 to S.M. and A.A., NSF grants no. DEB-0103794 and 0743890 to F.K., and by the Naomi Foundation through the Tel Aviv University GRTF programme grant no. 064181317 to A.S. K.T. and S.C. were supported by grants CGL2015-70390-P and PGC2018-098290-B-I00 (co-funded by FEDER) from the Spanish government. Fieldwork in Papua New Guinea and research permits were approved by the respective provincial governments, PNG National Research Institute, and the PNG Conservation and Environment Protection Authority. Finally, and most importantly, this work could not have been done without the generous assistance of many local communities in Papua New Guinea. We extend our deepest gratitude to the numerous landowners and field assistants who provided us with access to their lands and aided us in collections in the field.

FIGURE LEGENDS

Figure 1. Map of New Guinea showing the distribution of samples analysed herein and the type localities of recognized species of *Papuascincus*. The blue polygon includes all areas encompassing the elevational range of samples in this study (1190-3282 m), representing potential distribution for *Papuascincus*. Black dots denote sampled localities in this study. The red star denotes the type locality of *Papuascincus stanleyanus* (Mt. Victoria), the yellow star denotes the type locality of *Papuascincus morokanus* (Moroka), and the green dashed line follows the path of the Sepik River, the type locality for *Papuascincus buergersi* and *P. phaeodes*.

Figure 2. (A) a map of specimen localities used in the study. Overlaid on top of the map are polygons showing the distribution ranges of the Eastern and the Western clades in the phylogeny, inferred based on the sampled localities and their elevational range (1190-3282 m). The four different geological regions of Papua New Guinea are coloured blue (Australian Craton), purple (Fold Belt), green (Oceanic Arc Terranes), and yellow (East-Papuan Composite Terrane). (B) Bayesian Inference phylogenetic tree based on the concatenated dataset of three mitochondrial and two nuclear markers, with BI posterior probabilities and ML bootstrap support values shown at each node, respectively. On each label, the sample code of the specimen detailed in Table S1 is followed by a locality number presented in the map in panel A. Next to the tree are lineages as delimited by species delimitation methods: GMYC/bGMYC and BP&P. (C) Nuclear haplotype networks for two markers, *NGFB* (top) and *R35* (bottom). The colours correspond to the nine BP&P lineages as shown in panel B. Photo of *Papuascincus* courtesy of Allen Allison.

Figure 3. Time-calibrated phylogenetic trees and the ancestral biogeographical reconstruction analyses of *Papuascincus*. The analyses were based on the reduced concatenated dataset, containing a single sample per GMYC/bGMYC lineage, and an additional sample for lineage T (with a different elevational distribution). Branch colours and pie charts near the major nodes describe the probability of each inferred character state. (A) Reconstruction according to geological regions: blue (Australian Craton), purple (Fold Belt), green (Oceanic Arc Terranes), and yellow (East-Papuan Composite Terrane). Mean age estimates are provided above the nodes with horizontal bars representing the 95% highest posterior densities. (B) Reconstruction according to elevational distribution: brown (lower montane, 1000-1500 m), red (higher montane, 1500-2500 m), dark blue (subalpine, 2500-3000 m), and light blue (apine, > 3000m). Posterior probability values are indicated above the nodes.

Figure 4. Body size differentiation within *Papuascincus*. (A) Phenogram showing evolution of SVL along the time-calibrated phylogeny of 20 GMYC/bGMYC delimited lineages of *Papuascincus*, with blue colouration representing 95% confidence interval. Photos of *Papuascincus* specimens from the 'large' morph (top) and 'small' morph (bottom) courtesy of Allen Allison. (B) Boxplots of SVL for each GMYC/bGMYC delimited lineage. The boxplots are coloured based on BP&P delimited lineages.

650 **Figure 1.**

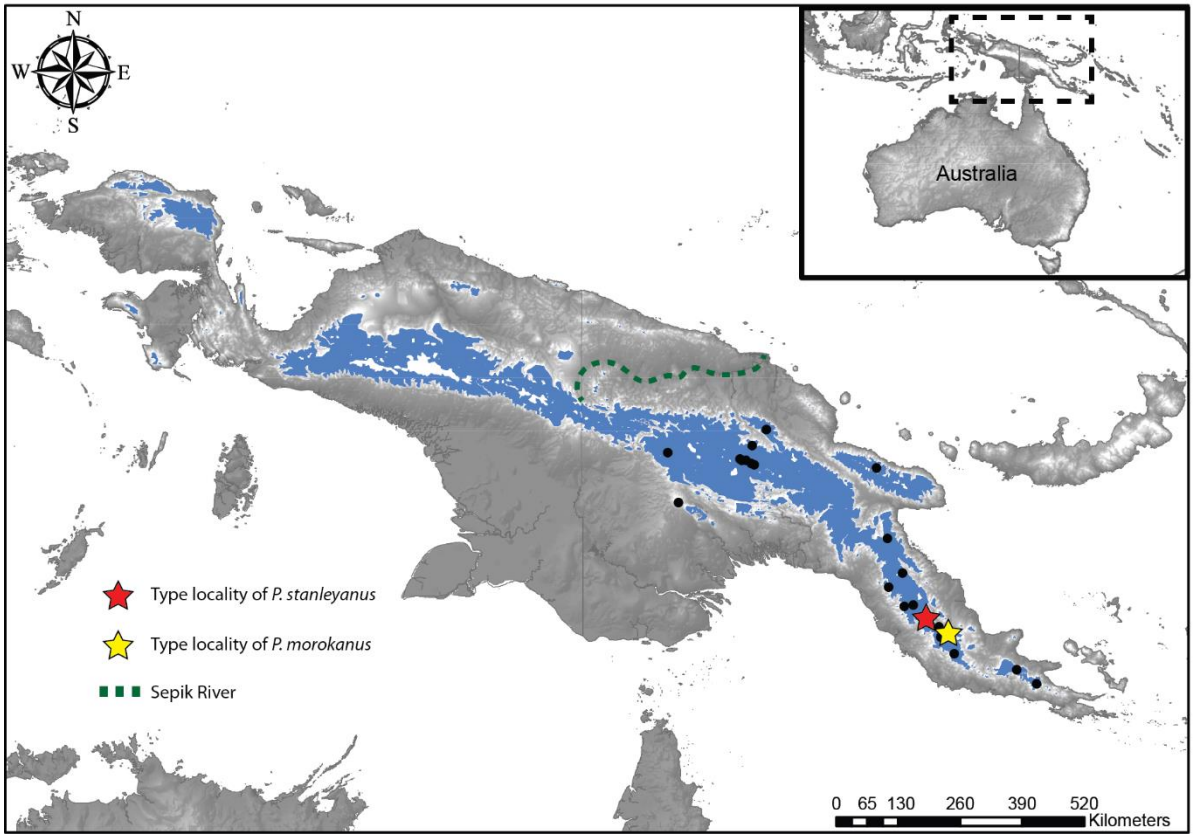

651

652 **Figure 2.**

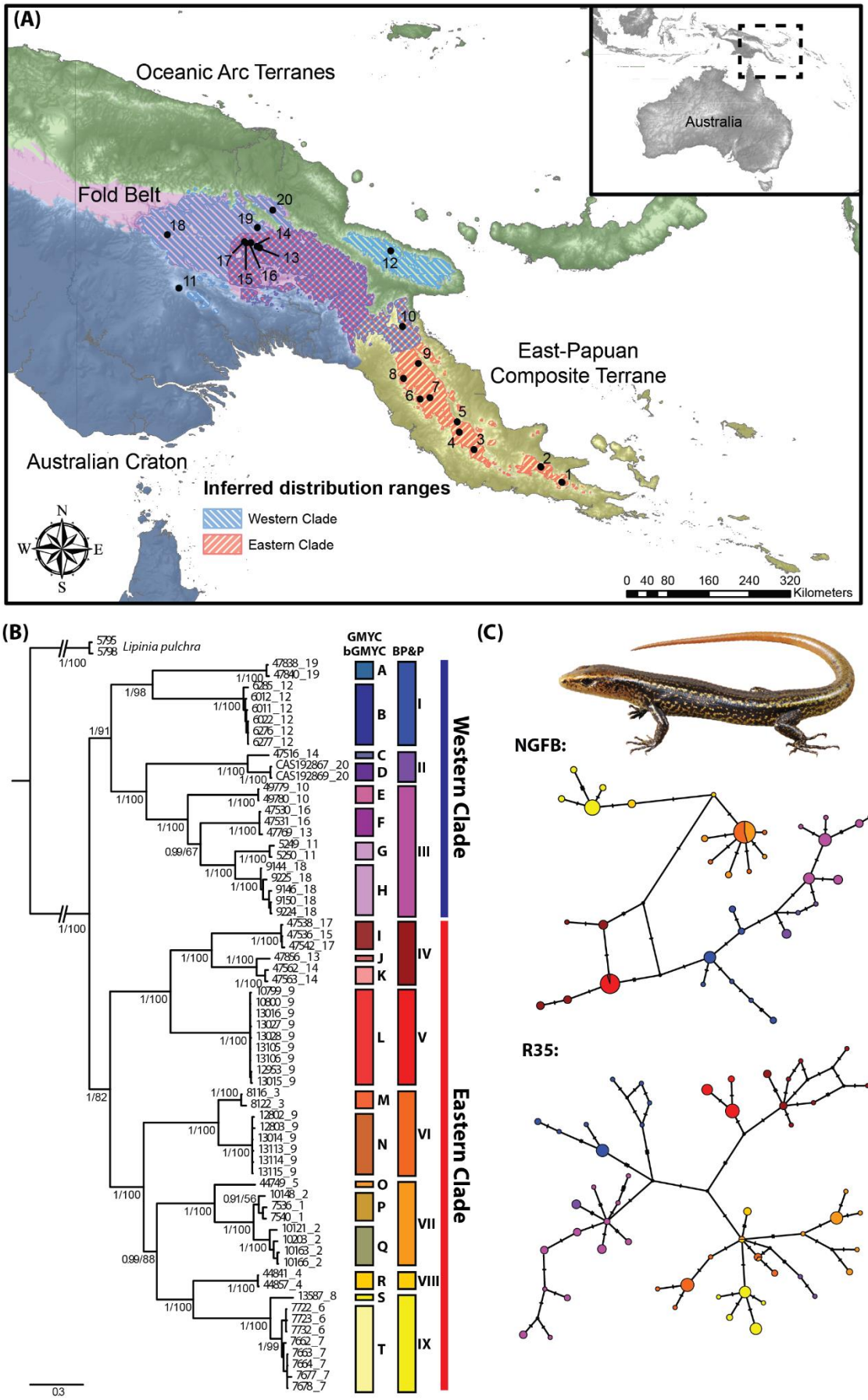
(A)
Oceanic Arc Terranes
Australia
Fold Belt
East-Papuan
Composite Terrane
Australian Craton
Inferred distribution ranges
Western Clade
Eastern Clade
N
W
E
S
0 40 80 160 240 320
Kilometers
(B)
Lipinia pulchra
GMYC
bGMYC
BP&P
Western Clade
Eastern Clade
(C)
NGFB:
R35:

654 **Figure 3.**

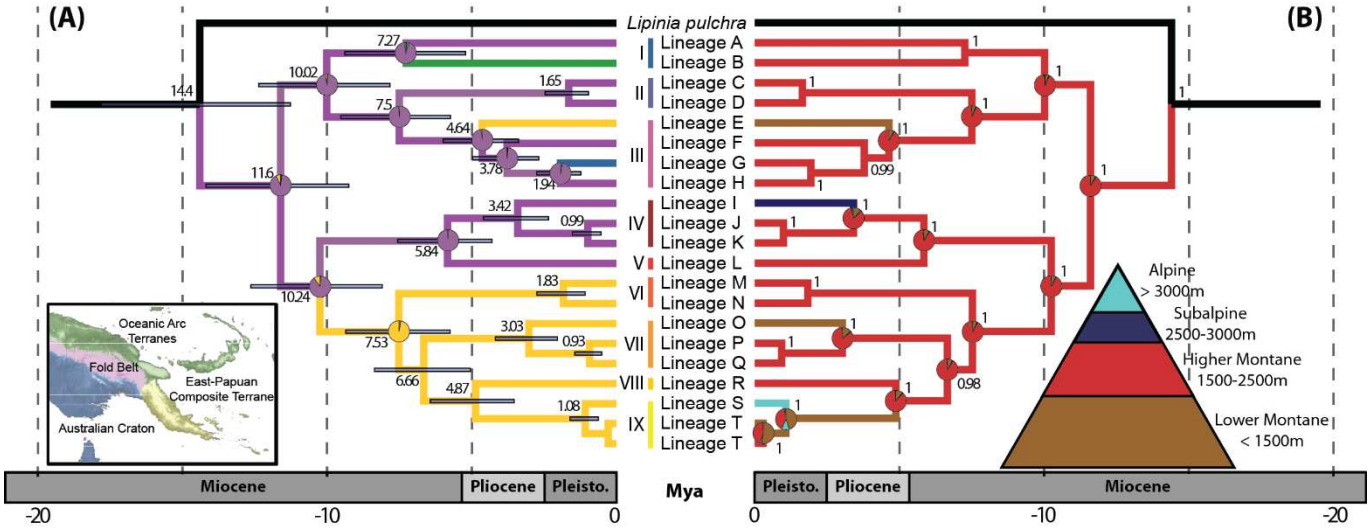

655

Figure 4.

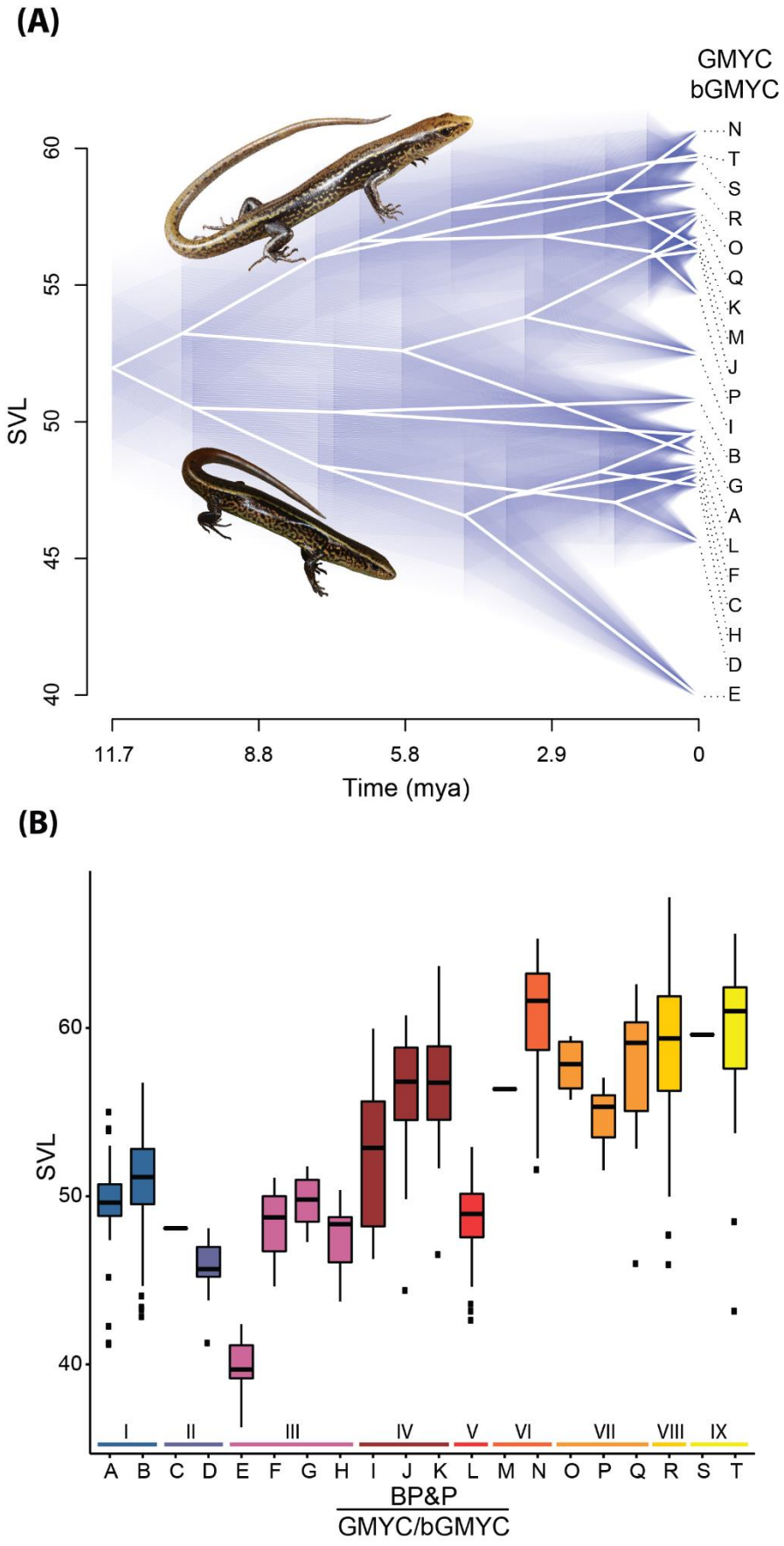
(A)
GMYC
bGMYC
N
T
S
R
O
Q
K
M
J
P
I
B
G
A
L
F
C
H
D
E
SVL
60
55
50
45
40
11.7
8.8
5.8
2.9
0
Time (mya)
(B)
SVL
60
50
40
I
II
III
IV
V
VI
VII
VIII
IX
A B C D E F G H I J K L M N O P Q R S T
BP&P
GMYC/bGMYC

SUPPLEMENTARY FILES

Figure S1. Maximum-likelihood phylogenetic tree based on the concatenated dataset of three mitochondrial and two nuclear markers, with BI posterior probabilities and ML bootstrap support values shown at each node, respectively. On each label, the number following the underscore corresponds to a locality in the map in Fig. 1A. Next to the tree are lineages as delimited by species delimitation methods: GMYC/bGMYC and BP&P.

Figure S2. Bayesian-inference phylogenetic trees based on the (A) concatenated mitochondrial dataset, and (B) concatenated nuclear dataset. BI posterior probabilities and ML bootstrap support values shown at each node, respectively. On each label, the number following the underscore corresponds to a locality in the map in Fig. 1A. Next to the trees are lineages as delimited by species delimitation methods: GMYC/bGMYC and BP&P.

Figure S3. Results of the GMYC and bGMYC analyses. (A) Clustering of samples into lineages according to GMYC, with each red clade representing a separate lineage. (B) Likelihood values produced by GMYC analysis to estimate the transition between interspecific diversification and allele intraspecific coalescence along the branches. (C) Lineage through time plot by GMYC analysis show in vertical red line the sharp increase in branching rate (threshold separating a Yule process from a Coalescent process). (D) Posterior distribution of lineage numbers according to bGMYC. The highest posterior probability is for 20 lineages.

Figure S4. Nuclear haplotype networks for two markers, *NGFB* (top) and *R35* (bottom). The colours correspond to the 20 GMYC/bGMYC lineages.

Figure S5. Time-calibrated phylogeny of *Papuascincus*. Mean age estimates are provided above the nodes with horizontal bars representing the 95% highest posterior densities. Posterior probability values are indicated next to the nodes. Details of the samples are presented in Table S1.

Figure S6. Phenogram showing evolution of SVL along the time-calibrated phylogeny of nine BP&P delimited lineages of *Papuascincus*, with blue colouration representing 95% confidence interval.

Figure S1.

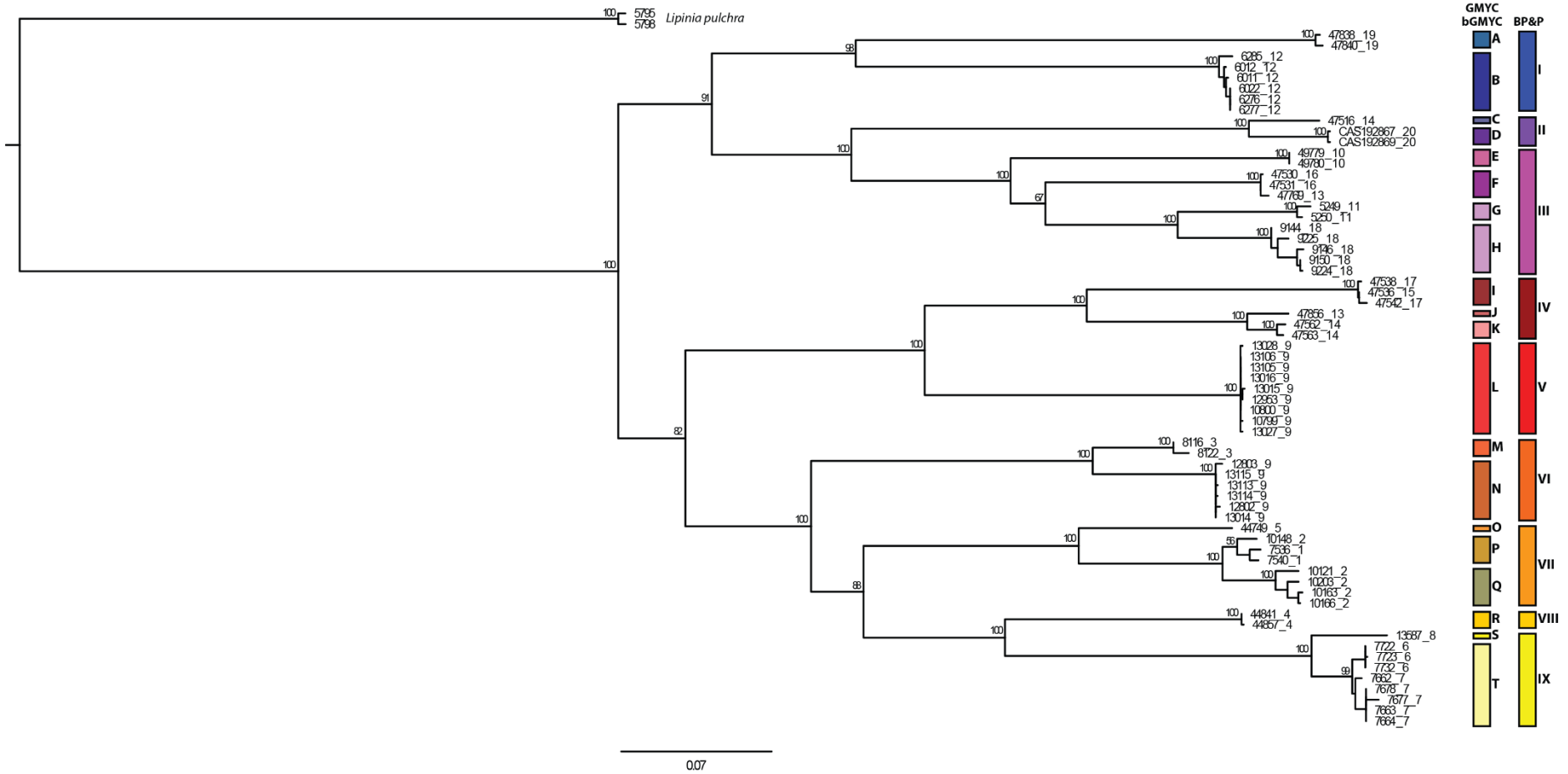
5795
5798
Lipinia pulchra
47838_19
47840_19
6285_12
6012_12
6011_12
6022_12
6276_12
6277_12
47516_14
CAS192867_20
CAS192869_20
49779_10
49780_10
47530_16
47531_16
47769_13
5249_11
5250_11
9144_18
9225_18
9146_18
9150_18
9224_18
47538_17
47536_15
47542_17
47856_13
47562_14
47563_14
13028_9
13106_9
13105_9
13016_9
13015_9
12963_9
10800_9
10799_9
13027_9
8116_3
8122_3
12803_9
13115_9
13113_9
13114_9
12802_9
13014_9
44749_5
10148_2
7536_1
7540_1
10121_2
10203_2
10163_2
10166_2
44841_4
44857_4
13587_8
7722_6
7723_6
7732_6
7662_7
7678_7
7677_7
7663_7
7664_7
0.07
GMYC
bGMYC
BP&P
A
B
C
D
E
F
G
H
I
J
K
L
M
N
O
P
Q
R
S
T
I
II
III
IV
V
VI
VII
VIII
IX

Figure S2.

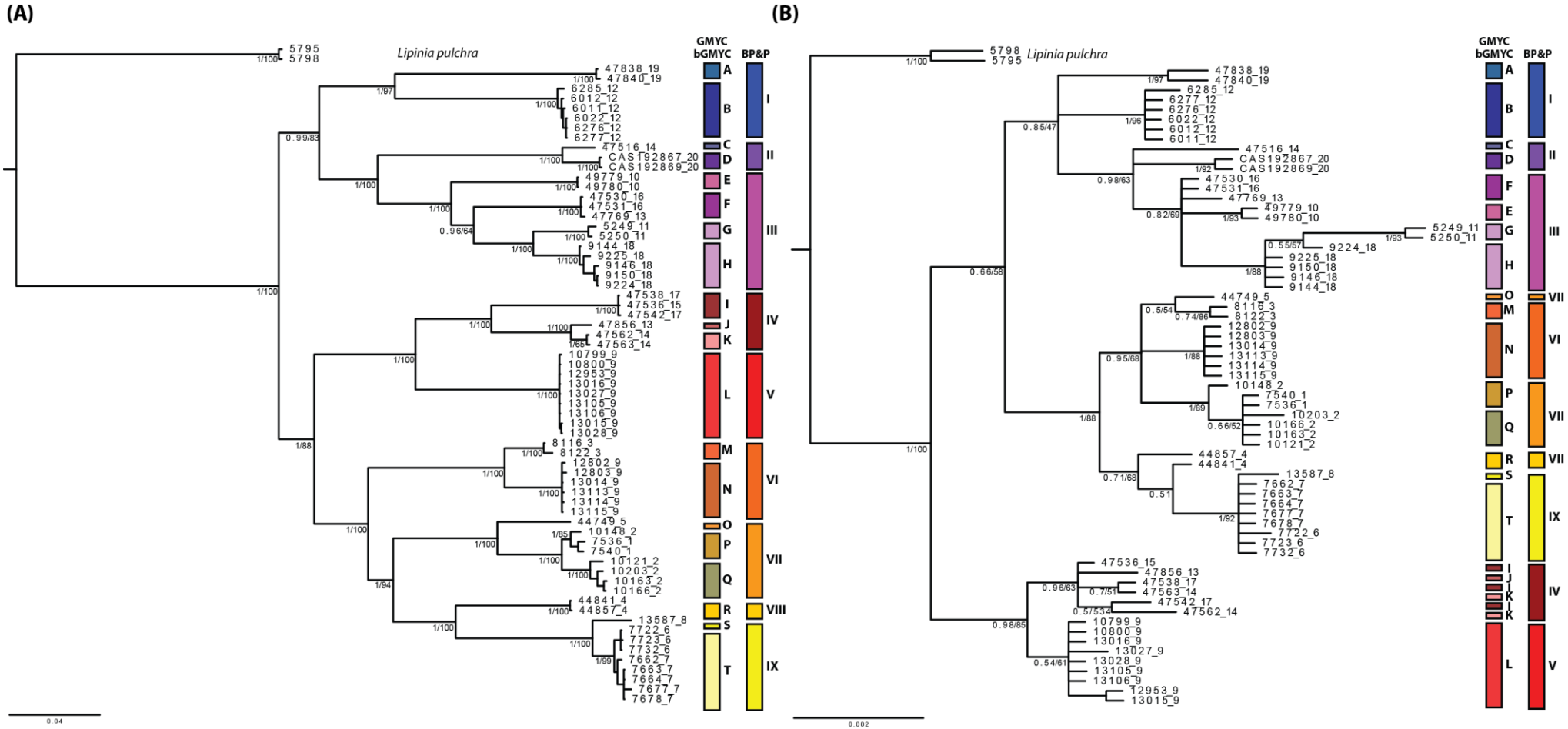

Figure S3.

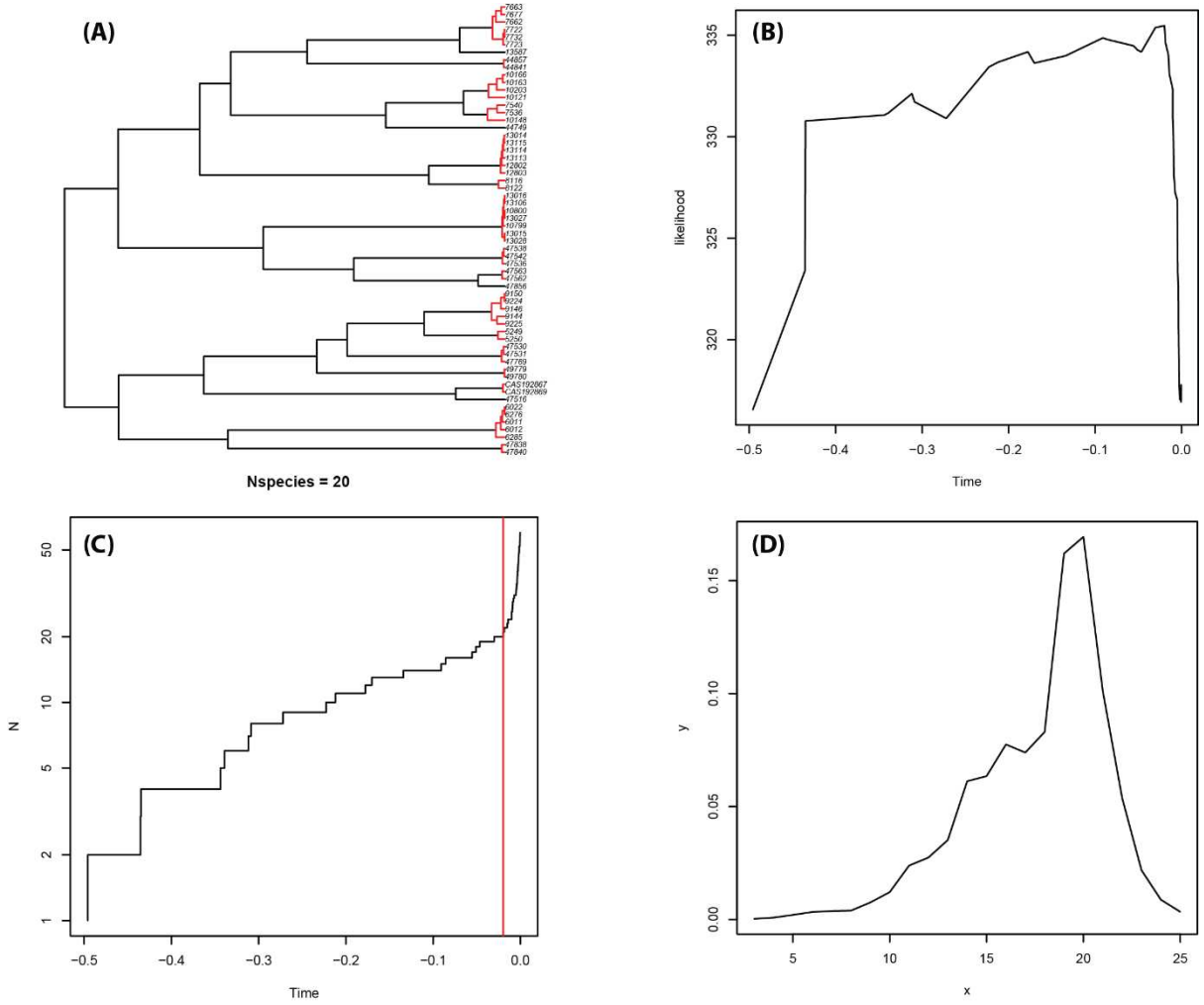

Figure S4.

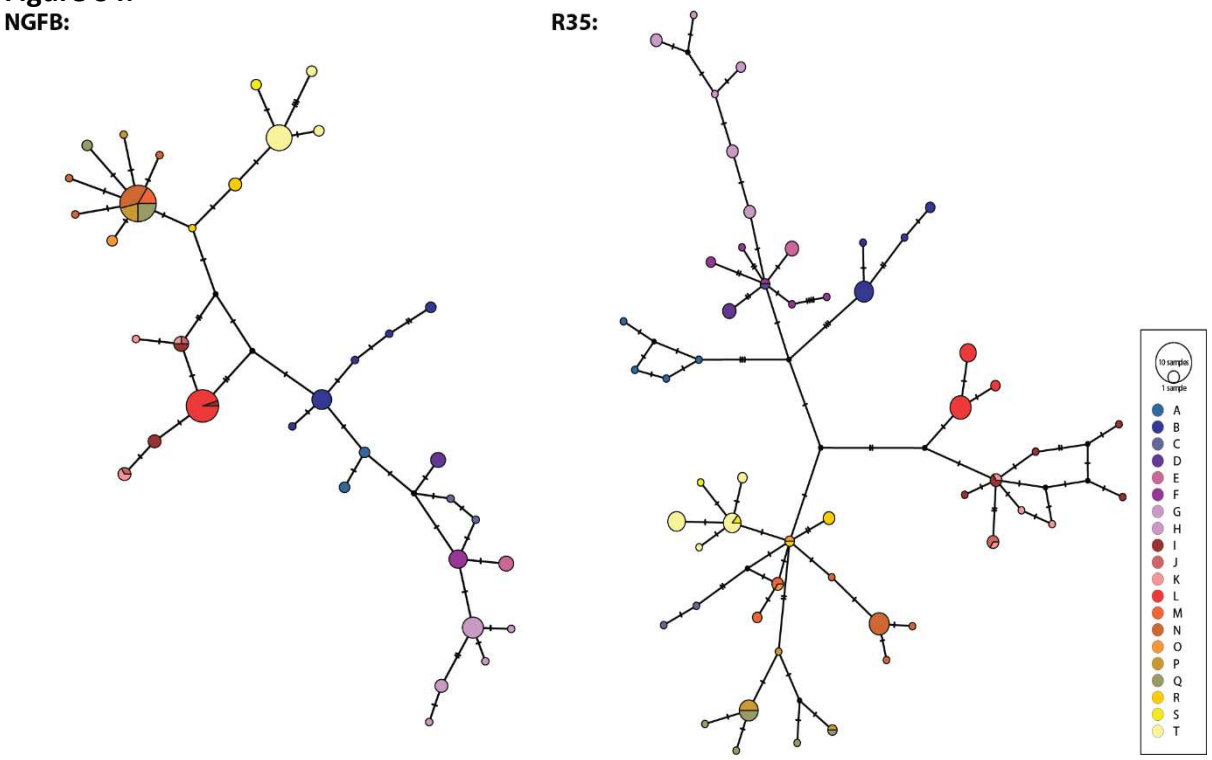

Figure S5.

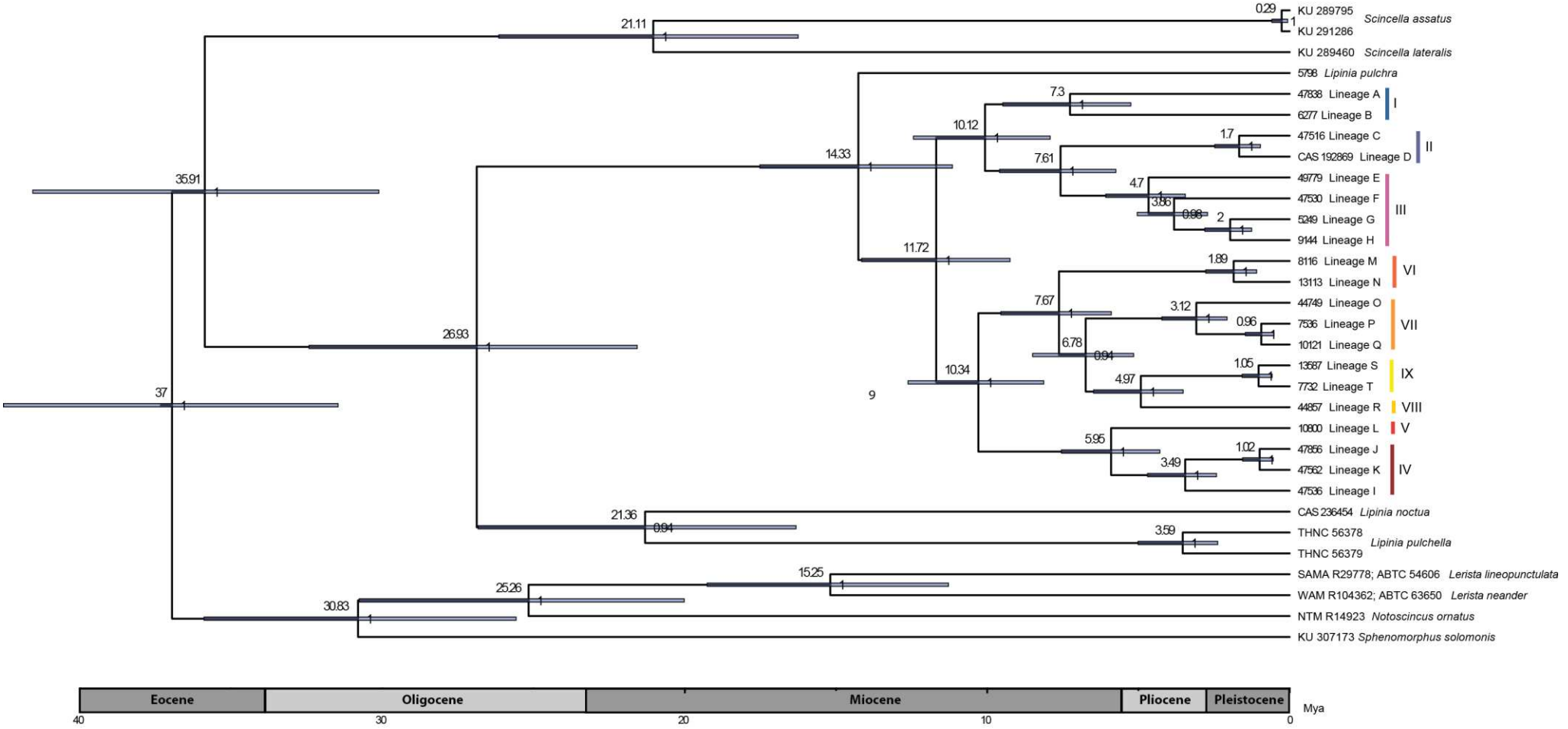
KU 289795 Scincella assatus
KU 291286
KU 289460 Scincella lateralis
5798 Lipinia pulchra
47838 Lineage A
6277 Lineage B
47516 Lineage C
CAS 192869 Lineage D
49779 Lineage E
47530 Lineage F
5249 Lineage G
9144 Lineage H
8116 Lineage M
13113 Lineage N
44749 Lineage O
7536 Lineage P
10121 Lineage Q
13587 Lineage S
7732 Lineage T
44857 Lineage R
10800 Lineage L
47866 Lineage J
47562 Lineage K
47536 Lineage I
CAS 236454 Lipinia noctua
THNC 56378
THNC 56379
Lipinia pulchella
SAMA R29778; ABTC 54606 Lerista lineopunctulata
WAM R104362; ABTC 63650 Lerista neander
NTM R14923 Notoscincus ornatus
KU 307173 Sphenomorphus solomonis
I
II
III
VI
VII
IX
VIII
V
IV
21.11
35.91
37
26.93
14.33
11.72
10.12
7.3
7.61
1.7
4.7
3.86
0.88
2
1.89
7.67
3.12
0.96
6.78
0.94
10.34
1.05
4.97
5.95
1.02
3.49
9
21.36
0.94
3.59
15.25
25.26
30.83
0.29
1
Eocene
Oligocene
Miocene
Pliocene
Pleistocene
Mya
40
30
20
10
0

Figure S6.

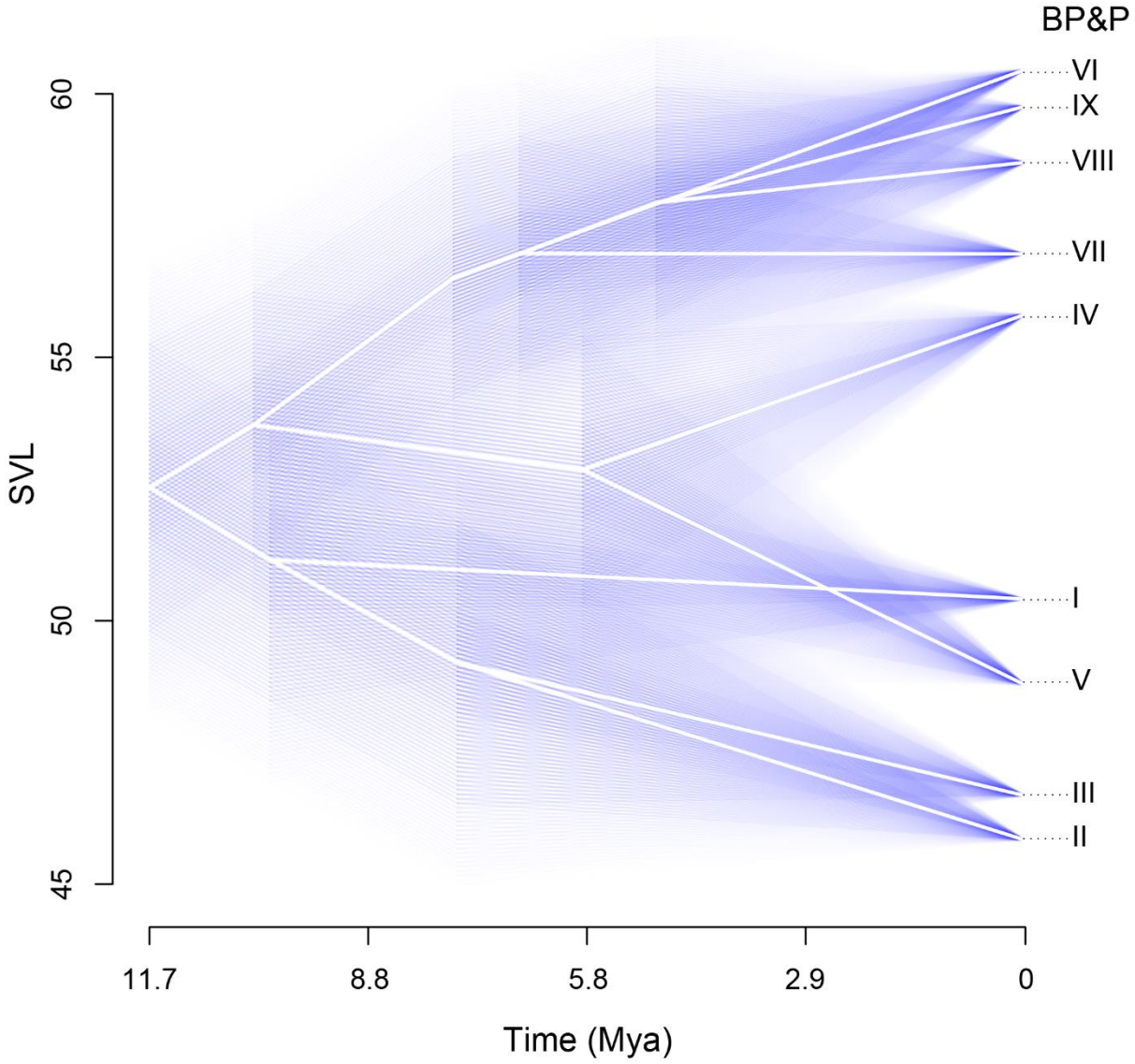
BP&P
VI
IX
VIII
VII
IV
I
V
III
II
SVL
60
55
50
45
11.7
8.8
5.8
2.9
0
Time (Mya)

Table S1. Information on the specimens included in this study and related GenBank accession numbers. Tissue codes correspond to the labels assigned to each sample in the phylogenetic analyses. For *Papuascincus* specimens, information in the "species" column is given regarding phylogenetic clades denoted by species delimitation methods (GMYC/bGMYC: letters A-T, BP&P: Roman numerals I-IX, respectively) and locality data (as shown in Figure 1A). SVL (in mm) of voucher specimens and elevation (in m) of the locality are listed for specimens used in biogeographic reconstruction and size evolution analyses. [a] Mitochondrial Haplotypes used for the GMYC and bGMYC species delimitation analyses (n=60). [b] Representatives used for estimation of divergence times and ancestral state reconstructions (n=32). * Juvenile specimen omitted from body size comparisons (n=3).

Tissue Code	Voucher Code	Species	SVL	Elevation	Locality	Latitude	Longitude	*12S*	*ND2*	*ND4*	*NGFB*	*R35*
5249 [a,b]	BPBM 34851	*Papuascincus* G III	50.7	2443	11	-6.6143	142.8267	MN870695	MN870760	MN870825	MN870890	MN870955
5250 [a]	BPBM 34852	*Papuascincus* G III	48.9	2443	11	-6.6143	142.8267	MN870696	MN870761	MN870826	MN870891	MN870956
6011 [a]	BPBM 40404	*Papuascincus* B I	48.6	2173	12	-5.9552	146.5595	MN870699	MN870764	MN870829	MN870894	MN870959
6012 [a]	BPBM 40405	*Papuascincus* B I	50.4	2173	12	-5.9552	146.5595	MN870700	MN870765	MN870830	MN870895	MN870960
6022 [a]	BPBM 40397	*Papuascincus* B I	50.8	2655	12	-5.9372	146.5503	MN870701	MN870766	MN870831	MN870896	MN870961
6276 [a]	BPBM 40450	*Papuascincus* B I	56.7	2556	12	-5.9392	146.5523	MN870702	MN870767	MN870832	MN870897	MN870962
6277 [b]	BPBM 40449	*Papuascincus* B I	51.6	2556	12	-5.9392	146.5523	MN870703	MN870768	MN870833	MN870898	MN870963
6285 [a]	BPBM 40445	*Papuascincus* B I	54.8	2646	12	-5.9358	146.5574	MN870704	MN870769	MN870834	MN870899	MN870964
7536 [a,b]	BPBM 16767	*Papuascincus* P VII	56	2480	1	-10.0364	149.5749	MN870705	MN870770	MN870835	MN870900	MN870965
7540 [a]	BPBM 16769	*Papuascincus* P VII	53.5	2480	1	-10.0364	149.5749	MN870706	MN870771	MN870836	MN870901	MN870966
7662 [a]	BPBM 18858	*Papuascincus* T IX	60.9	1620	7	-8.5378	147.2423	MN870707	MN870772	MN870837	MN870902	MN870967
7663 [a]	BPBM 18859	*Papuascincus* T IX	57.1	1620	7	-8.5378	147.2423	MN870708	MN870773	MN870838	MN870903	MN870968
7664	BPBM 18860	*Papuascincus* T IX	41.1*	1650	7	-8.5291	147.2345	MN870709	MN870774	MN870839	MN870904	MN870969
7677 [a]	BPBM 18861	*Papuascincus* T IX	52.2	1604	7	-8.5448	147.2505	MN870710	MN870775	MN870840	MN870905	MN870970
7678	BPBM 18862	*Papuascincus* T IX	57.4	1604	7	-8.5448	147.2505	MN870711	MN870776	MN870841	MN870906	MN870971
7722 [a]	BPBM 18875	*Papuascincus* T IX	52.4	1800	6	-8.5693	147.0768	MN870712	MN870777	MN870842	MN870907	MN870972
7723 [a]	BPBM 18876	*Papuascincus* T IX	57.4	1800	6	-8.5693	147.0768	MN870713	MN870778	MN870843	MN870908	MN870973
7732 [a,b]	BPBM 18881	*Papuascincus* T IX	58.2	1340	6	-8.5683	147.0851	MN870714	MN870779	MN870844	MN870909	MN870974
8116 [a,b]	BPBM 19591	*Papuascincus* M VI	56.4	1822	3	-9.4571	148.0258	MN870715	MN870780	MN870845	MN870910	MN870975
8122 [a]	BPBM 19593	*Papuascincus* M VI	43.8*	1822	3	-9.4571	148.0258	MN870716	MN870781	MN870846	MN870911	MN870976
9144 [a,b]	BPBM 34179	*Papuascincus* H III	48.6	2177	18	-5.6695	142.6233	MN870717	MN870782	MN870847	MN870912	MN870977
9146 [a]	BPBM 34180	*Papuascincus* H III	44.6	1910	18	-5.6431	142.6342	MN870718	MN870783	MN870848	MN870913	MN870978
9150 [a]	BPBM 34181	*Papuascincus* H III	48.3	1910	18	-5.6431	142.6342	MN870719	MN870784	MN870849	MN870914	MN870979
9224 [a]	BPBM 34186	*Papuascincus* H III	47	2351	18	-5.6668	142.6163	MN870720	MN870785	MN870850	MN870915	MN870980
9225 [a]	BPBM 34187	*Papuascincus* H III	48.7	2351	18	-5.6668	142.6163	MN870721	MN870786	MN870851	MN870916	MN870981
10121 [a, b]	BPBM 39060	*Papuascincus* Q VII	52.8	1730	2	-9.7651	149.2176	MN870662	MN870727	MN870792	MN870857	MN870922
10148 [a]	BPBM 39061	*Papuascincus* P VII	57	1860	2	-9.7580	149.1822	MN870663	MN870728	MN870793	MN870858	MN870923
10163 [a]	BPBM 39063	*Papuascincus* Q VII	62.6	1860	2	-9.7580	149.1822	MN870664	MN870729	MN870794	MN870859	MN870924
10166 [a]	BPBM 39071	*Papuascincus* Q VII	59.7	1790	2	-9.7626	149.2021	MN870665	MN870730	MN870795	MN870860	MN870925
10203 [a]	BPBM 39089	*Papuascincus* Q VII	60.6	1730	2	-9.7651	149.2176	MN870666	MN870731	MN870796	MN870861	MN870926
10799 [a]	BPBM 38211	*Papuascincus* L V	49.2	1737	9	-7.9188	147.0843	MN870667	MN870732	MN870797	MN870862	MN870927

Tissue Code	Voucher Code	Species	SVL	Elevation	Locality	Latitude	Longitude	*12S*	*ND2*	*ND4*	*NGFB*	*R35*
10800 [a,b]	BPBM 38206	*Papuascincus* L V	47.1	1737	9	-7.9188	147.0843	MN870668	MN870733	MN870798	MN870863	MN870928
12802 [a]	BPBM 41228	*Papuascincus* N VI	62.5	1856	9	-7.9210	147.0802	MN870669	MN870734	MN870799	MN870864	MN870929
12803 [a]	BPBM 41229	*Papuascincus* N VI	61.2	1856	9	-7.9210	147.0802	MN870670	MN870735	MN870800	MN870865	MN870930
12953	BPBM 41253	*Papuascincus* L V	51.3	1856	9	-7.9210	147.0802	MN870671	MN870736	MN870801	MN870866	MN870931
13014 [a]	BPBM 41245	*Papuascincus* N VI	51.6	1733	9	-7.9372	147.0544	MN870672	MN870737	MN870802	MN870867	MN870932
13015 [a]	BPBM 41256	*Papuascincus* L V	48.8	1733	9	-7.9372	147.0544	MN870673	MN870738	MN870803	MN870868	MN870933
13016 [a]	BPBM 41257	*Papuascincus* L V	48.2	1733	9	-7.9372	147.0544	MN870674	MN870739	MN870804	MN870869	MN870934
13027 [a]	BPBM 41267	*Papuascincus* L V	48.6	1965	9	-7.9380	147.0458	MN870675	MN870740	MN870805	MN870870	MN870935
13028 [a]	BPBM 41268	*Papuascincus* L V	49.2	1965	9	-7.9380	147.0458	MN870676	MN870741	MN870806	MN870871	MN870936
13105	BPBM 41300	*Papuascincus* L V	49.4	2161	9	-7.9325	147.0399	MN870677	MN870742	MN870807	MN870872	MN870937
13106 [a]	BPBM 41301	*Papuascincus* L V	52.9	2161	9	-7.9325	147.0399	MN870678	MN870743	MN870808	MN870873	MN870938
13113 [a,b]	BPBM 41246	*Papuascincus* N VI	63.7	1965	9	-7.9380	147.0458	MN870679	MN870744	MN870809	MN870874	MN870939
13114 [a]	BPBM 41247	*Papuascincus* N VI	61.4	2161	9	-7.9325	147.0399	MN870680	MN870745	MN870810	MN870875	MN870940
13115 [a]	BPBM 41248	*Papuascincus* N VI	57.3	2161	9	-7.9325	147.0399	MN870681	MN870746	MN870811	MN870876	MN870941
13587 [a,b]	BPBM 44306	*Papuascincus* S IX	59.6	3282	8	-8.2069	146.7848	MN870682	MN870747	MN870812	MN870877	MN870942
44749 [a,b]	BPBM 44749	*Papuascincus* O VII	59.5	1262	5	-8.9646	147.7327	MN870722	MN870787	MN870852	MN870917	MN870982
44841 [a]	BPBM 44841	*Papuascincus* R VIII	63.6	1936	4	-9.1288	147.7264	MN870723	MN870788	MN870853	MN870918	MN870983
44857 [a,b]	BPBM 44857	*Papuascincus* R VIII	64.8	2076	4	-9.1509	147.7675	MN870724	MN870789	MN870854	MN870919	MN870984
47516 [a,b]	BPBM 22896	*Papuascincus* C II	48.1	1800	14	-5.8735	144.2003	MN870683	MN870748	MN870813	MN870878	MN870943
47530 [a,b]	BPBM 22902	*Papuascincus* F III	45.9	2200	16	-5.8120	144.0950	MN870684	MN870749	MN870814	MN870879	MN870944
47531 [a]	BPBM 22903	*Papuascincus* F III	50	2200	16	-5.8120	144.0950	MN870685	MN870750	MN870815	MN870880	MN870945
47536 [a,b]	BPBM 22908	*Papuascincus* I IV	60	2600	15	-5.8193	144.0144	MN870686	MN870751	MN870816	MN870881	MN870946
47538 [a]	BPBM 22910	*Papuascincus* I IV	46.3	2800	17	-5.7935	143.9799	MN870687	MN870752	MN870817	MN870882	MN870947
47542 [a]	BPBM 22914	*Papuascincus* I IV	43.6*	2800	17	-5.7935	143.9799	MN870688	MN870753	MN870818	MN870883	MN870948
47562 [a,b]	BPBM 22934	*Papuascincus* K IV	57	1800	14	-5.8735	144.2003	MN870689	MN870754	MN870819	MN870884	MN870949
47563 [a]	BPBM 22935	*Papuascincus* K IV	56.7	1800	14	-5.8735	144.2033	MN870690	MN870755	MN870820	MN870885	MN870950
47769 [a]	BPBM 47769	*Papuascincus* F III	44.6	1960	13	-5.8991	144.2521	MN870726	MN870791	MN870856	MN870921	MN870986
47838 [a,b]	BPBM 23082	*Papuascincus* A I	50.1	1650	19	-5.5423	144.2091	MN870691	MN870756	MN870821	MN870886	MN870951
47840 [a]	BPBM 23084	*Papuascincus* A I	48.7	1650	19	-5.5423	144.2091	MN870692	MN870757	MN870822	MN870887	MN870952
47856 [a,b]	BPBM 47856	*Papuascincus* J IV	60.1	1960	13	-5.8991	144.2521	MN870725	MN870790	MN870855	MN870920	MN870985
49779 [a,b]	BPBM 23713	*Papuascincus* E III	41.1	1190	10	-7.2885	146.7654	MN870693	MN870758	MN870823	MN870888	MN870953
49780 [a]	BPBM 23714	*Papuascincus* E III	42.1	1190	10	-7.2885	146.7654	MN870694	MN870759	MN870824	MN870889	MN870954
CAS 192867 [a]	CAS 192687	*Papuascincus* D II	48.1	1830	20	-5.2376	144.4805	JF497876	JF498128	JF498479	JF498234	JF498355
CAS 192869 [a,b]	CAS 192869	*Papuascincus* D II	43.8	1830	20	-5.2376	144.4805	JF497877	JF498129	JF498480	JF498235	JF498356
CAS 236454 [b]	CAS 236454	*Lipinia noctua*	-	-	-	-	-	JF497868	JF498120	JF498473	-	JF498348
THNC 56378 [b]		*Lipinia pulchella*	-	-	-	-	-	JF497869	JF498121	JF498474	JF498228	JF498349
THNC 56379 [b]		*Lipinia pulchella*	-	-	-	-	-	JF497870	JF498122	JF498475	JF498229	-
5795 [b]	BPBM 38789	*Lipinia pulchra*	-	-	-	-	-	MN870697	MN870762	MN870827	MN870892	MN870957
5798 [b]	BPBM 38792	*Lipinia pulchra*	-	-	-	-	-	MN870698	MN870763	MN870828	MN870893	MN870958
SAMA R29778; ABTC 54606 [b]		*Lerista lineopunctulata*	-	-	-	-	-	EF672792	JQ517871	EF673004	-	-
WAM R104362;		*Lerista neander*	-	-	-	-	-	EF672796	-	EF673008	-	-

Tissue Code	Voucher Code	Species	SVL	Elevation	Locality	Latitude	Longitude	*12S*	*ND2*	*ND4*	*NGFB*	*R35*
ABTC 63650 [b]												
NTM R14923		*Notoscincus ornatus*	-	-	-	-	-	AY169594	-	AY169669	-	-
KU 289795 [b]		*Scincella assatus*	-	-	-	-	-	JF497946	-	JF498548	JF498302	JF498427
KU 291286 [b]		*Scincella assatus*	-	-	-	-	-	-	JF498186	JF498549	JF498303	JF498428
KU 289460 [b]		*Scincella lateralis*	-	-	-	-	-	JF497948	JF498187	AY169673	JF498305	JF498430
KU 307173 [b]		*Sphenomorphus solomonis*	-	-	-	-	-	JF497964	JF498203	JF498567	JF498321	JF498446

Table S2. Specimens used for body size analyses. Tissue code is given for voucher specimens of samples used in the molecular analyses. SVL was recorded to the nearest 0.1 mm.

Voucher Code	Collection Code	Tissue Code	GMYC/bGMYC	BP&P	SVL (mm)	Latitude	Longitude
BPBM 23071	AA 12174		A	I	49.7	-5.542282	144.209116
BPBM 23072	AA 12175		A	I	47.9	-5.542282	144.209116
BPBM 23073	AA 12176		A	I	49.3	-5.542282	144.209116
BPBM 23074	AA 12177		A	I	49.5	-5.542282	144.209116
BPBM 23075	AA 12178		A	I	50.9	-5.542282	144.209116
BPBM 23076	AA 12179		A	I	49.1	-5.542282	144.209116
BPBM 23077	AA 12180		A	I	49.5	-5.542282	144.209116
BPBM 23078	AA 12181		A	I	41.2	-5.542282	144.209116
BPBM 23079	AA 12182		A	I	51.5	-5.542282	144.209116
BPBM 23080	AA 12183		A	I	50.8	-5.542282	144.209116
BPBM 23081	AA 12184		A	I	50.6	-5.542282	144.209116
BPBM 23082	AA 12185	47838	A	I	50.1	-5.542282	144.209116
BPBM 23083	AA 12186		A	I	48.2	-5.542282	144.209116
BPBM 23084	AA 12187	47840	A	I	48.7	-5.542282	144.209116
BPBM 23085	AA 12188		A	I	50.2	-5.542282	144.209116
BPBM 23086	AA 12189		A	I	49.7	-5.542282	144.209116
BPBM 23087	AA 12190		A	I	48.9	-5.542282	144.209116
BPBM 23088	AA 12191		A	I	50.7	-5.542282	144.209116
BPBM 23089	AA 12192		A	I	45.2	-5.542282	144.209116
BPBM 30503	AA 10899		A	I	54.0	-5.533	144.15
BPBM 30504	AA 10900		A	I	48.9	-5.533	144.15
BPBM 30505	AA 10901		A	I	42.3	-5.533	144.15
BPBM 30506	AA 10902		A	I	50.1	-5.533	144.15
BPBM 30556	AA 10958		A	I	49.4	-5.509057999	144.1621552
BPBM 30605	AA 11025		A	I	52.1	-5.542282	144.209116
BPBM 30606	AA 11026		A	I	47.8	-5.542282	144.209116
BPBM 30607	AA 11027		A	I	50.2	-5.542282	144.209116

BPBM 30610	AA 11030		A	I	41.3	-5.542282	144.209116
BPBM 30611	AA 11031		A	I	49.5	-5.542282	144.209116
BPBM 30612	AA 11032		A	I	50.0	-5.542282	144.209116
BPBM 30613	AA 11033		A	I	48.8	-5.542282	144.209116
BPBM 30614	AA 11034		A	I	55.0	-5.542282	144.209116
BPBM 30615	AA 11035		A	I	49.6	-5.542282	144.209116
BPBM 30616	AA 11036		A	I	53.0	-5.542282	144.209116
BPBM 30617	AA 11037		A	I	50.4	-5.542282	144.209116
BPBM 30618	AA 11038		A	I	48.8	-5.542282	144.209116
BPBM 30619	AA 11039		A	I	50.8	-5.542282	144.209116
BPBM 30620	AA 11040		A	I	48.3	-5.542282	144.209116
BPBM 30621	AA 11041		A	I	50.1	-5.542282	144.209116
BPBM 30622	AA 11042		A	I	53.0	-5.542282	144.209116
BPBM 30623	AA 11043		A	I	53.9	-5.542282	144.209116
BPBM 30624	AA 11044		A	I	47.4	-5.542282	144.209116
BPBM 30625	AA 11045		A	I	49.0	-5.542282	144.209116
BPBM 30626	AA 11046		A	I	49.6	-5.542282	144.209116
BPBM 30627	AA 11047		A	I	50.7	-5.542282	144.209116
BPBM 30628	AA 11048		A	I	52.3	-5.542282	144.209116
BPBM 40378	AA 20321		B	I	48.7	-5.95517	146.55952
BPBM 40379	AA 20316		B	I	50.7	-5.95517	146.55952
BPBM 40380	AA 20323		B	I	49.7	-5.95517	146.55952
BPBM 40381	AA 20325		B	I	44.1	-5.95517	146.55952
BPBM 40383	AA 20322		B	I	50.7	-5.95517	146.55952
BPBM 40384	AA 20443		B	I	51.7	-5.95517	146.55952
BPBM 40385	AA 20320		B	I	53.3	-5.95517	146.55952
BPBM 40386	AA 20319		B	I	52.0	-5.95517	146.55952
BPBM 40387	AA 20327		B	I	49.4	-5.95517	146.55952
BPBM 40388	AA 20317		B	I	49.6	-5.95517	146.55952

BPBM 40391	AA 20314		B	I	47.0	-5.95517	146.55952
BPBM 40392	AA 20313		B	I	52.7	-5.95517	146.55952
BPBM 40394	AA 20311		B	I	43.4	-5.95517	146.55952
BPBM 40395	AA 20310		B	I	48.7	-5.95517	146.55952
BPBM 40396	AA 20284		B	I	45.7	-5.95517	146.55952
BPBM 40397	AA 20294	6022	B	I	50.8	-5.93721	146.55032
BPBM 40400	AA 20358		B	I	49.8	-5.95517	146.55952
BPBM 40401	AA 20357		B	I	50.6	-5.95517	146.55952
BPBM 40402	AA 20356		B	I	52.1	-5.95517	146.55952
BPBM 40404	AA 20282	6011	B	I	48.6	-5.95517	146.55952
BPBM 40405	AA 20283	6012	B	I	50.4	-5.95517	146.55952
BPBM 40407	AA 20326		B	I	53.3	-5.95517	146.55952
BPBM 40408	AA 20344		B	I	51.0	-5.95517	146.55952
BPBM 40409	AA 20436		B	I	52.7	-5.95517	146.55952
BPBM 40414	AA 20337		B	I	51.1	-5.95517	146.55952
BPBM 40417	AA 20329		B	I	51.2	-5.95517	146.55952
BPBM 40418	AA 20345		B	I	44.7	-5.95517	146.55952
BPBM 40419	AA 20484		B	I	54.0	-5.95517	146.55952
BPBM 40421	AA 20496		B	I	54.8	-5.95517	146.55952
BPBM 40422	AA 20495		B	I	53.3	-5.95517	146.55952
BPBM 40423	AA 20494		B	I	50.2	-5.95517	146.55952
BPBM 40424	AA 20493		B	I	52.5	-5.95517	146.55952
BPBM 40425	AA 20491		B	I	54.8	-5.95517	146.55952
BPBM 40428	AA 20488		B	I	51.5	-5.95517	146.55952
BPBM 40431	AA 20485		B	I	53.9	-5.95517	146.55952
BPBM 40433	AA 20483		B	I	55.0	-5.95517	146.55952
BPBM 40434	AA 20482		B	I	46.6	-5.95517	146.55952
BPBM 40435	AA 20481		B	I	52.2	-5.95517	146.55952
BPBM 40436	AA 20480		B	I	53.4	-5.95517	146.55952

BPBM 40437	AA 20479		B	I	47.8	-5.95517	146.55952
BPBM 40438	AA 20478		B	I	53.3	-5.95517	146.55952
BPBM 40439	AA 20477		B	I	50.2	-5.95517	146.55952
BPBM 40440	AA 20476		B	I	54.1	-5.95517	146.55952
BPBM 40441	AA 20441		B	I	54.5	-5.95517	146.55952
BPBM 40442	AA 20474		B	I	48.3	-5.95517	146.55952
BPBM 40443	AA 20486		B	I	52.1	-5.95517	146.55952
BPBM 40445	AA 20575	6285	B	I	54.8	-5.93577	146.55735
BPBM 40448	AA 20568		B	I	51.7	-5.93919	146.55229
BPBM 40449	AA 20567	6277	B	I	51.6	-5.93919	146.55229
BPBM 40450	AA 20566	6276	B	I	56.7	-5.93919	146.55229
BPBM 40454	AA 20492		B	I	42.8	-5.95517	146.55952
BPBM 40457	AA 20473		B	I	51.4	-5.95517	146.55952
BPBM 40459	AA 20454		B	I	46.4	-5.95517	146.55952
BPBM 40461	AA 20506		B	I	46.7	-5.95517	146.55952
BPBM 40462	AA 20505		B	I	47.2	-5.95517	146.55952
BPBM 40463	AA 20504		B	I	49.8	-5.95517	146.55952
BPBM 40464	AA 20503		B	I	47.1	-5.95517	146.55952
BPBM 40465	AA 20502		B	I	47.4	-5.95517	146.55952
BPBM 40466	AA 20501		B	I	50.3	-5.95517	146.55952
BPBM 40469	AA 20431		B	I	47.5	-5.95517	146.55952
BPBM 40473	AA 20442		B	I	50.6	-5.95517	146.55952
BPBM 40474	AA 20440		B	I	52.0	-5.95517	146.55952
BPBM 40475	AA 20439		B	I	50.1	-5.95517	146.55952
BPBM 40476	AA 20438		B	I	46.3	-5.95517	146.55952
BPBM 40477	AA 20437		B	I	52.8	-5.95517	146.55952
BPBM 40478	AA 20435		B	I	48.2	-5.95517	146.55952
BPBM 40480	AA 20472		B	I	51.6	-5.95517	146.55952
BPBM 40482	AA 20446		B	I	43.3	-5.95517	146.55952

BPBM 40483	AA 20430		B	I	51.1	-5.95517	146.55952
BPBM 40484	AA 20429		B	I	47.5	-5.95517	146.55952
BPBM 40485	AA 20428		B	I	50.0	-5.95517	146.55952
BPBM 40486	AA 20427		B	I	49.7	-5.95517	146.55952
BPBM 40487	AA 20426		B	I	52.8	-5.95517	146.55952
BPBM 40488	AA 20425		B	I	54.3	-5.95517	146.55952
BPBM 40489	AA 20424		B	I	53.1	-5.95517	146.55952
BPBM 40490	AA 20423		B	I	53.1	-5.95517	146.55952
BPBM 40494	AA 20459		B	I	45.8	-5.95517	146.55952
BPBM 40495	AA 20471		B	I	52.6	-5.95517	146.55952
BPBM 40496	AA 20470		B	I	51.1	-5.95517	146.55952
BPBM 40497	AA 20469		B	I	49.6	-5.95517	146.55952
BPBM 40498	AA 20468		B	I	50.2	-5.95517	146.55952
BPBM 40499	AA 20467		B	I	52.4	-5.95517	146.55952
BPBM 40500	AA 20466		B	I	49.5	-5.95517	146.55952
BPBM 40501	AA 20465		B	I	54.3	-5.95517	146.55952
BPBM 40502	AA 20464		B	I	50.4	-5.95517	146.55952
BPBM 40503	AA 20463		B	I	49.9	-5.95517	146.55952
BPBM 40504	AA 20462		B	I	48.1	-5.95517	146.55952
BPBM 40505	AA 20461		B	I	52.0	-5.95517	146.55952
BPBM 40506	AA 20444		B	I	50.7	-5.95517	146.55952
BPBM 40507	AA 20460		B	I	54.6	-5.95517	146.55952
BPBM 40509	AA 20458		B	I	55.1	-5.95517	146.55952
BPBM 40510	AA 20457		B	I	52.0	-5.95517	146.55952
BPBM 40511	AA 20456		B	I	50.9	-5.95517	146.55952
BPBM 40512	AA 20455		B	I	51.5	-5.95517	146.55952
BPBM 40513	AA 20453		B	I	53.0	-5.95517	146.55952
BPBM 40514	AA 20452		B	I	48.6	-5.95517	146.55952
BPBM 40515	AA 20451		B	I	52.1	-5.95517	146.55952

BPBM 40516	AA 20450		B	I	52.7	-5.95517	146.55952
BPBM 40517	AA 20449		B	I	51.8	-5.95517	146.55952
BPBM 40518	AA 20448		B	I	53.9	-5.95517	146.55952
SAM R69660	2159		B	I	54.0	-6.079	146.575
SAM R69663	2174		B	I	55.3	-6.079	146.575
SAM R69664	2192		B	I	49.9	-6.079	146.575
SAM R69668	2202		B	I	53.4	-6.097	146.559
SAM R69670	2214		B	I	54.2	-6.097	146.559
SAM R69671	2215		B	I	51.4	-6.097	146.559
BPBM 22896	AA 11485	47516	C	II	48.1	-5.87345413	144.2003064
CAS 192866	RNF 0064		D	II	47.1	-5.2376	144.4805
CAS 192867	RNF 0065	CAS192867	D	II	48.1	-5.2376	144.4805
CAS 192868	RNF 0066		D	II	47.3	-5.2376	144.4805
CAS 192869	RNF 0067	CAS192869	D	II	43.8	-5.2376	144.4805
CAS 192870	RNF 0068		D	II	45.1	-5.2376	144.4805
CAS 192871	RNF 0069		D	II	45.4	-5.2376	144.4805
CAS 192872	RNF 0070		D	II	46.0	-5.2376	144.4805
CAS 192874	RNF 0075		D	II	45.7	-5.2376	144.4805
CAS 192875	RNF 0076		D	II	46.8	-5.2376	144.4805
CAS 192876	RNF 0078		D	II	45.4	-5.2376	144.4805
CAS 192877	RNF 0080		D	II	41.3	-5.2376	144.4805
BPBM 23647	AA 12801		E	III	39.2	-7.2789858	146.7744565
BPBM 23682	AA 12951		E	III	39.5	-7.2826087	146.7690217
BPBM 23713	AA 13047	49779	E	III	41.1	-7.2884963	146.7653985
BPBM 23714	AA 13048	49780	E	III	42.1	-7.2884963	146.7653985
BPBM 23715	AA 13049		E	III	40.6	-7.2884963	146.7653985
BPBM 24060	AA 12760		E	III	38.8	-7.2826087	146.7690217
BPBM 24061	AA 12761		E	III	39.7	-7.2826087	146.7690217
BPBM 24063	AA 12767		E	III	36.3	-7.2826087	146.7690217
BPBM 24064	AA 12772		E	III	42.4	-7.2826087	146.7690217

BPBM 22902	AA 11505	47530	F	III	45.9	-5.812	144.095
BPBM 22903	AA 11506	47531	F	III	50.0	-5.812	144.095
BPBM 22904	AA 11507		F	III	51.1	-5.812	144.095
BPBM 22905	AA 11508		F	III	51.1	-5.812	144.095
BPBM 22906	AA 11509		F	III	46.0	-5.812	144.095
BPBM 22907	AA 11510		F	III	48.7	-5.812	144.095
BPBM 22966	AA 11606		F	III	48.8	-5.812	144.095
BPBM 22967	AA 11607		F	III	48.7	-5.812	144.095
BPBM 22968	AA 11608		F	III	50.7	-5.812	144.095
BPBM 22969	AA 11609		F	III	48.5	-5.812	144.095
BPBM 22970	AA 11610		F	III	46.7	-5.812	144.095
BPBM 22971	AA 11611		F	III	50.3	-5.812	144.095
BPBM 22972	AA 11612		F	III	46.3	-5.812	144.095
BPBM 22973	AA 11613		F	III	49.1	-5.812	144.095
BPBM 22974	AA 11614		F	III	49.1	-5.812	144.095
BPBM 22975	AA 11615		F	III	46.9	-5.812	144.095
BPBM 47769	AA 24811	47769	F	III	44.6	-5.8991	144.2521
BPBM 34851	AA 19399	5249	G	III	50.7	-6.614342	142.826652
BPBM 34852	AA 19400	5250	G	III	48.9	-6.614342	142.826652
BPBM 34853	AA 19401		G	III	47.3	-6.614342	142.826652
BPBM 34854	AA 19402		G	III	51.8	-6.614342	142.826652
BPBM 34179	FK 12506	9144	H	III	48.6	-5.66954	142.62334
BPBM 34180	FK 12508	9146	H	III	44.6	-5.6431	142.6342
BPBM 34181	FK 12512	9150	H	III	48.3	-5.6431	142.6342
BPBM 34182	FK 12513		H	III	50.4	-5.6431	142.6342
BPBM 34183	FK 12514		H	III	43.7	-5.6431	142.6342
BPBM 34184	FK 12544		H	III	48.6	-5.65915	142.63538
BPBM 34185	FK 12545		H	III	48.7	-5.65915	142.63538
BPBM 34186	FK 12721	9224	H	III	47.0	-5.66681	142.61625
BPBM 34187	FK 12722	9225	H	III	48.7	-5.66681	142.61625

BPBM 34189	FK 12746		H	III	48.0	-5.65915	142.63538
BPBM 34192	FK 12775		H	III	49.4	-5.68381	142.61012
BPBM 34193	FK 12776		H	III	48.9	-5.68381	142.61012
BPBM 34194	FK 12777		H	III	46.1	-5.68381	142.61012
BPBM 34195	FK 12778		H	III	45.4	-5.68381	142.61012
BPBM 34203	FK 12811		H	III	45.8	-5.67075	142.62553
BPBM 34204	FK 12812		H	III	48.4	-5.67075	142.62553
BPBM 34206	FK 12814		H	III	47.2	-5.67075	142.62553
BPBM 34207	FK 12815		H	III	46.0	-5.67075	142.62553
BPBM 34215	FK 12905		H	III	50.2	-5.66465	142.61949
	FK 12543		H	III	49.4	-5.6592	142.635
BPBM 22908	AA 11511	47536	I	IV	60.0	-5.819347	144.014407
BPBM 22910	AA 11515	47538	I	IV	46.3	-5.793534	143.979889
BPBM 22915	AA 11520		I	IV	55.4	-5.793534	143.979889
BPBM 22916	AA 11521		I	IV	55.7	-5.793534	143.979889
BPBM 22920	AA 11525		I	IV	51.0	-5.793534	143.979889
BPBM 22921	AA 11526		I	IV	47.7	-5.793534	143.979889
BPBM 22924	AA 11529		I	IV	47.6	-5.793534	143.979889
BPBM 22925	AA 11530		I	IV	46.9	-5.793534	143.979889
BPBM 22928	AA 11533		I	IV	50.6	-5.793534	143.979889
BPBM 22979	AA 11621		I	IV	49.9	-5.793534	143.979889
BPBM 22981	AA 11623		I	IV	56.9	-5.793534	143.979889
BPBM 22983	AA 11625		I	IV	54.7	-5.793534	143.979889
BPBM 22985	AA 11627		I	IV	54.7	-5.793534	143.979889
BPBM 22986	AA 11628		I	IV	57.7	-5.793534	143.979889
BPBM 22898	AA 11501		J	IV	59.5	-5.812	144.095
BPBM 22901	AA 11504		J	IV	57.6	-5.812	144.095
BPBM 22911	AA 11516		J	IV	54.3	-5.793534	143.979889
BPBM 22913	AA 11518		J	IV	44.4	-5.793534	143.979889

BPBM 22918	AA 11523		J	IV	55.3	-5.793534	143.979889
BPBM 22919	AA 11524		J	IV	53.7	-5.793534	143.979889
BPBM 22922	AA 11527		J	IV	56.7	-5.793534	143.979889
BPBM 22923	AA 11528		J	IV	51.2	-5.793534	143.979889
BPBM 22926	AA 11531		J	IV	58.3	-5.793534	143.979889
BPBM 22936	AA 11546		J	IV	60.3	-5.87345413	144.2003064
BPBM 22944	AA 11584		J	IV	56.3	-5.812	144.095
BPBM 22946	AA 11586		J	IV	60.8	-5.812	144.095
BPBM 22947	AA 11587		J	IV	54.8	-5.812	144.095
BPBM 22949	AA 11589		J	IV	56.3	-5.812	144.095
BPBM 22950	AA 11590		J	IV	56.8	-5.812	144.095
BPBM 22954	AA 11594		J	IV	60.3	-5.812	144.095
BPBM 22955	AA 11595		J	IV	50.8	-5.812	144.095
BPBM 22956	AA 11596		J	IV	59.4	-5.812	144.095
BPBM 22959	AA 11599		J	IV	55.3	-5.812	144.095
BPBM 22960	AA 11600		J	IV	57.7	-5.812	144.095
BPBM 22963	AA 11603		J	IV	58.0	-5.812	144.095
BPBM 22964	AA 11604		J	IV	55.1	-5.812	144.095
BPBM 22978	AA 11620		J	IV	52.8	-5.793534	143.979889
BPBM 22984	AA 11626		J	IV	58.3	-5.793534	143.979889
BPBM 22987	AA 11629		J	IV	49.8	-5.793534	143.979889
BPBM 23023	AA 11879		J	IV	58.7	-5.827355	144.045508
BPBM 23025	AA 11881		J	IV	53.1	-5.615138	143.880914
BPBM 23030	AA 11886		J	IV	57.2	-5.615138	143.880914
BPBM 23031	AA 11887		J	IV	59.4	-5.615138	143.880914
BPBM 23032	AA 11888		J	IV	58.3	-5.615138	143.880914
BPBM 23033	AA 11889		J	IV	54.1	-5.615138	143.880914
BPBM 23036	AA 11892		J	IV	59.0	-5.615138	143.880914
BPBM 23043	AA 11899		J	IV	56.1	-5.615138	143.880914

BPBM 23044	AA 11900		J	IV	59.4	-5.615138	143.880914
BPBM 47856	AA 24898	47856	J	IV	60.1	-5.899058	144.252075
BPBM 22900	AA 11503		K	IV	55.8	-5.812	144.095
BPBM 22934	AA 11544	47562	K	IV	57.0	-5.87345413	144.2003064
BPBM 22935	AA 11545	47563	K	IV	56.7	-5.87345413	144.2003064
BPBM 22938	AA 11578		K	IV	54.8	-5.812	144.095
BPBM 22939	AA 11579		K	IV	59.2	-5.812	144.095
BPBM 22940	AA 11580		K	IV	56.1	-5.812	144.095
BPBM 22941	AA 11581		K	IV	59.4	-5.812	144.095
BPBM 22942	AA 11582		K	IV	58.4	-5.812	144.095
BPBM 22943	AA 11583		K	IV	56.0	-5.812	144.095
BPBM 22945	AA 11585		K	IV	63.7	-5.812	144.095
BPBM 22948	AA 11588		K	IV	51.9	-5.812	144.095
BPBM 22951	AA 11591		K	IV	58.5	-5.812	144.095
BPBM 22953	AA 11593		K	IV	63.7	-5.812	144.095
BPBM 22957	AA 11597		K	IV	53.4	-5.812	144.095
BPBM 22958	AA 11598		K	IV	56.2	-5.812	144.095
BPBM 22965	AA 11605		K	IV	59.1	-5.812	144.095
BPBM 23018	AA 11874		K	IV	62.8	-5.827355	144.045508
BPBM 23019	AA 11875		K	IV	54.7	-5.827355	144.045508
BPBM 23020	AA 11876		K	IV	62.0	-5.827355	144.045508
BPBM 23021	AA 11877		K	IV	51.9	-5.827355	144.045508
BPBM 23022	AA 11878		K	IV	56.8	-5.827355	144.045508
BPBM 23028	AA 11884		K	IV	60.1	-5.615138	143.880914
BPBM 23037	AA 11893		K	IV	53.5	-5.615138	143.880914
BPBM 23038	AA 11894		K	IV	59.9	-5.615138	143.880914
BPBM 23039	AA 11895		K	IV	46.5	-5.615138	143.880914
BPBM 23040	AA 11896		K	IV	57.1	-5.615138	143.880914
BPBM 23045	AA 11901		K	IV	51.7	-5.615138	143.880914

BPBM 2575			K	IV	52.9	-5.869196	144.763327
BPBM 30564	AA 10979		K	IV	58.1	-5.8269016	144.0205562
BPBM 30565	AA 10980		K	IV	57.2	-5.8269016	144.0205562
BPBM 30566	AA 10981		K	IV	58.8	-5.8269016	144.0205562
BPBM 30571	AA 10986		K	IV	57.1	-5.8269016	144.0205562
BPBM 30572	AA 10989		K	IV	55.9	-5.8269016	144.0205562
BPBM 30576	AA 10993		K	IV	54.4	-5.8269016	144.0205562
BPBM 30577	AA 10994		K	IV	53.3	-5.8269016	144.0205562
BPBM 38206	AA 20771	10800	L	V	47.1	-7.91876	147.08429
BPBM 38210	AA 20772		L	V	43.6	-7.91876	147.08429
BPBM 38211	AA 20770	10799	L	V	49.2	-7.91876	147.08429
BPBM 41250	AA 21175		L	V	49.7	-7.921	147.08015
BPBM 41251	AA 21177		L	V	48.5	-7.921	147.08015
BPBM 41253	AA 21310	12953	L	V	51.3	-7.921	147.08015
BPBM 41254	AA 21311		L	V	48.9	-7.921	147.08015
BPBM 41255	AA 21316		L	V	47.3	-7.921	147.08015
BPBM 41256	AA 21404	13015	L	V	48.8	-7.93721	147.05444
BPBM 41257	AA 21405	13016	L	V	48.2	-7.93721	147.05444
BPBM 41258	AA 21407		L	V	45.4	-7.93721	147.05444
BPBM 41259	AA 21408		L	V	50.3	-7.93721	147.05444
BPBM 41260	AA 21409		L	V	48.8	-7.93721	147.05444
BPBM 41262	AA 21411		L	V	43.2	-7.93721	147.05444
BPBM 41263	AA 21412		L	V	46.5	-7.93721	147.05444
BPBM 41264	AA 21413		L	V	50.3	-7.93721	147.05444
BPBM 41265	AA 21414		L	V	49.7	-7.93803	147.04582
BPBM 41266	AA 21415		L	V	51.4	-7.93803	147.04582
BPBM 41267	AA 21416	13027	L	V	48.6	-7.93803	147.04582
BPBM 41268	AA 21417	13028	L	V	49.2	-7.93803	147.04582
BPBM 41269	AA 21418		L	V	48.6	-7.93803	147.04582
BPBM 41271	AA 21420		L	V	50.1	-7.93803	147.04582

BPBM 41272	AA 21421		L	V	51.3	-7.93803	147.04582
BPBM 41273	AA 21422		L	V	47.5	-7.93803	147.04582
BPBM 41274	AA 21423		L	V	51.7	-7.93803	147.04582
BPBM 41275	AA 21424		L	V	49.9	-7.93803	147.04582
BPBM 41276	AA 21456		L	V	50.8	-7.93803	147.04582
BPBM 41277	AA 21457		L	V	50.2	-7.93803	147.04582
BPBM 41278	AA 21458		L	V	49.5	-7.93803	147.04582
BPBM 41279	AA 21459		L	V	42.6	-7.93803	147.04582
BPBM 41281	AA 21461		L	V	50.1	-7.93803	147.04582
BPBM 41284	AA 21464		L	V	46.4	-7.93803	147.04582
BPBM 41285	AA 21465		L	V	48.8	-7.93803	147.04582
BPBM 41286	AA 21466		L	V	49.6	-7.93803	147.04582
BPBM 41287	AA 21467		L	V	50.1	-7.93803	147.04582
BPBM 41289	AA 21469		L	V	46.5	-7.93803	147.04582
BPBM 41290	AA 21470		L	V	48.6	-7.93803	147.04582
BPBM 41291	AA 21471		L	V	45.9	-7.93803	147.04582
BPBM 41292	AA 21472		L	V	48.7	-7.93803	147.04582
BPBM 41293	AA 21473		L	V	51.6	-7.93803	147.04582
BPBM 41294	AA 21474		L	V	48.9	-7.93803	147.04582
BPBM 41295	AA 21475		L	V	45.0	-7.93803	147.04582
BPBM 41297	AA 21477		L	V	50.5	-7.93803	147.04582
BPBM 41298	AA 21478		L	V	47.0	-7.93803	147.04582
BPBM 41300	AA 21495	13105	L	V	49.4	-7.93251	147.03993
BPBM 41301	AA 21496	13106	L	V	52.9	-7.93251	147.03993
BPBM 41303	AA 21526		L	V	49.0	-7.93803	147.04582
BPBM 41304	AA 21527		L	V	44.6	-7.93803	147.04582
BPBM 41306	AA 21529		L	V	48.3	-7.93803	147.04582
BPBM 41308	AA 21531		L	V	50.9	-7.93803	147.04582
BPBM 41309	AA 21532		L	V	48.4	-7.93803	147.04582

BPBM 41310	AA 21533		L	V	48.8	-7.93803	147.04582
BPBM 41311	AA 21534		L	V	47.2	-7.93803	147.04582
BPBM 41312	AA 21535		L	V	47.6	-7.93803	147.04582
BPBM 41314	AA 21542		L	V	45.4	-7.93721	147.05444
BPBM 41315	AA 21560		L	V	52.3	-7.93721	147.05444
BPBM 41316	AA 21561		L	V	49.5	-7.93721	147.05444
BPBM 41317	AA 21562		L	V	49.3	-7.93721	147.05444
BPBM 41318	AA 21563		L	V	49.7	-7.93721	147.05444
BPBM 41319	AA 21564		L	V	51.8	-7.93721	147.05444
BPBM 41320	AA 21565		L	V	50.0	-7.93721	147.05444
BPBM 41321	AA 21566		L	V	51.0	-7.93721	147.05444
BPBM 41322	AA 21567		L	V	51.9	-7.93721	147.05444
BPBM 41323	AA 21406		L	V	48.3	-7.93721	147.05444
BPBM 19591	FK 8959	8116	M	VI	56.4	-9.45711	148.0258
BPBM 38212	AA 20733		N	VI	61.9	-7.91876	147.08429
BPBM 41227	AA 21136		N	VI	61.0	-7.921	147.08015
BPBM 41228	AA 21144	12802	N	VI	62.5	-7.921	147.08015
BPBM 41229	AA 21145	12803	N	VI	61.2	-7.921	147.08015
BPBM 41230	AA 21171		N	VI	58.5	-7.921	147.08015
BPBM 41231	AA 21172		N	VI	52.3	-7.921	147.08015
BPBM 41232	AA 21173		N	VI	63.7	-7.921	147.08015
BPBM 41233	AA 21174		N	VI	61.5	-7.921	147.08015
BPBM 41234	AA 21179		N	VI	63.4	-7.921	147.08015
BPBM 41235	AA 21202		N	VI	55.1	-7.921	147.08015
BPBM 41236	AA 21303		N	VI	65.3	-7.921	147.08015
BPBM 41237	AA 21304		N	VI	62.3	-7.921	147.08015
BPBM 41238	AA 21305		N	VI	61.7	-7.921	147.08015
BPBM 41239	AA 21306		N	VI	65.1	-7.921	147.08015
BPBM 41240	AA 21307		N	VI	64.1	-7.921	147.08015

BPBM 41241	AA 21308		N	VI	62.6	-7.921	147.08015
BPBM 41242	AA 21312		N	VI	58.1	-7.921	147.08015
BPBM 41243	AA 21313		N	VI	63.2	-7.921	147.08015
BPBM 41244	AA 21314		N	VI	59.1	-7.921	147.08015
BPBM 41245	AA 21403	13014	N	VI	51.6	-7.93721	147.05444
BPBM 41246	AA 21503	13113	N	VI	63.7	-7.93803	147.04582
BPBM 41247	AA 21504	13114	N	VI	61.4	-7.93251	147.03993
BPBM 41248	AA 21505	13115	N	VI	57.3	-7.93251	147.03993
BPBM 41249	AA 21506		N	VI	58.8	-7.93251	147.03993
BPBM 44747	AA 23018		O	VII	55.7	-8.9650667	147.73275
BPBM 44748	AA 23079		O	VII	56.6	-8.964611	147.732717
BPBM 44749	AA 23080	44749	O	VII	59.5	-8.964611	147.732717
BPBM 44750	AA 23134		O	VII	59.1	-8.96438	147.731923
BPBM 16767	FK 7409	7536	P	VII	56.0	-10.0364	149.5749
BPBM 16769	FK 7417	7540	P	VII	53.5	-10.0364	149.5749
BPBM 39061	FK 15334	10148	P	VII	57.0	-9.75802	149.18218
PM 25118	FK 7418		P	VII	51.5	-10.0364167	149.5748833
PM 25119	FK 7419		P	VII	55.3	-10.0364167	149.5748833
BPBM 39060	FK 15282	10121	Q	VII	52.8	-9.76505	149.21764
BPBM 39063	FK 15379	10163	Q	VII	62.6	-9.75802	149.18218
BPBM 39064	FK 15380		Q	VII	59.1	-9.75802	149.18218
BPBM 39069	FK 15385		Q	VII	46.0	-9.76258	149.20211
BPBM 39071	FK 15387	10166	Q	VII	59.7	-9.76258	149.20211
BPBM 39072	FK 15388		Q	VII	56.2	-9.76258	149.20211
BPBM 39081	FK 15409		Q	VII	61.0	-9.75802	149.18218
BPBM 39082	FK 15410		Q	VII	60.1	-9.75802	149.18218
BPBM 39083	FK 15411		Q	VII	60.9	-9.75802	149.18218
BPBM 39085	FK 15428		Q	VII	59.4	-9.75802	149.18218
BPBM 39086	FK 15429		Q	VII	58.6	-9.75802	149.18218
BPBM 39087	FK 15430		Q	VII	58.7	-9.75802	149.18218

BPBM 39088	FK 15431		Q	VII	53.2	-9.75802	149.18218
BPBM 39089	FK 15578	10203	Q	VII	60.6	-9.76505	149.21764
	FK 15397		Q	VII	54.0	-9.76258	149.20211
BPBM 44751	AA 23146		R	VIII	61.7	-9.05596	147.7368
BPBM 44754	AA 23149		R	VIII	56.5	-9.05451	147.75782
BPBM 44755	AA 23150		R	VIII	52.6	-9.05451	147.75782
BPBM 44756	AA 23151		R	VIII	60.8	-9.05451	147.75782
BPBM 44757	AA 23152		R	VIII	54.3	-9.05451	147.75782
BPBM 44758	AA 23153		R	VIII	61.1	-9.05451	147.75782
BPBM 44759	AA 23154		R	VIII	51.9	-9.05451	147.75782
BPBM 44760	AA 23155		R	VIII	59.5	-9.05451	147.75782
BPBM 44762	AA 23157		R	VIII	65.2	-9.071289	147.735211
BPBM 44763	AA 23158		R	VIII	53.7	-9.0448833	147.74095
BPBM 44766	AA 23170		R	VIII	55.8	-9.033287	147.739861
BPBM 44767	AA 23171		R	VIII	57.8	-9.033287	147.739861
BPBM 44770	AA 23174		R	VIII	50.2	-9.033287	147.739861
BPBM 44771	AA 23181		R	VIII	57.3	-9.0378167	147.74085
BPBM 44772	AA 23182		R	VIII	59.2	-9.03825	147.7410333
BPBM 44775	AA 23185		R	VIII	56.6	-9.0366	147.7410667
BPBM 44777	AA 23198		R	VIII	54.6	-9.05451	147.73782
BPBM 44778	AA 23199		R	VIII	59.3	-9.05451	147.73782
BPBM 44779	AA 23200		R	VIII	61.0	-9.05451	147.73782
BPBM 44780	AA 23201		R	VIII	62.6	-9.05451	147.73782
BPBM 44781	AA 23202		R	VIII	57.9	-9.05451	147.73782
BPBM 44783	AA 23204		R	VIII	50.7	-9.04782	147.73505
BPBM 44787	AA 23208		R	VIII	55.3	-9.05596	147.7368
BPBM 44788	AA 23209		R	VIII	61.9	-9.07094	147.7348
BPBM 44789	AA 23210		R	VIII	64.0	-9.06744	147.73532
BPBM 44790	AA 23211		R	VIII	65.0	-9.08285	147.76342

BPBM 44791	AA 23212		R	VIII	57.2	-9.08285	147.76342
BPBM 44792	AA 23215		R	VIII	58.1	-9.091225	147.734361
BPBM 44793	AA 23216		R	VIII	59.2	-9.091225	147.734361
BPBM 44794	AA 23217		R	VIII	59.5	-9.091225	147.734361
BPBM 44795	AA 23218		R	VIII	52.1	-9.091225	147.734361
BPBM 44797	AA 23220		R	VIII	59.5	-9.091225	147.734361
BPBM 44798	AA 23221		R	VIII	62.2	-9.091225	147.734361
BPBM 44799	AA 23222		R	VIII	59.3	-9.091225	147.734361
BPBM 44801	AA 23224		R	VIII	51.3	-9.091225	147.734361
BPBM 44802	AA 23225		R	VIII	55.0	-9.091225	147.734361
BPBM 44812	AA 23235		R	VIII	55.1	-9.091225	147.734361
BPBM 44813	AA 23236		R	VIII	50.0	-9.091225	147.734361
BPBM 44815	AA 23238		R	VIII	56.2	-9.091225	147.734361
BPBM 44817	AA 23242		R	VIII	63.1	-9.091225	147.734361
BPBM 44820	AA 23246		R	VIII	57.1	-9.091225	147.734361
BPBM 44821	AA 23247		R	VIII	55.2	-9.091225	147.734361
BPBM 44822	AA 23248		R	VIII	61.5	-9.091225	147.734361
BPBM 44824	AA 23250		R	VIII	52.0	-9.092002	147.7379
BPBM 44825	AA 23251		R	VIII	60.6	-9.092002	147.7379
BPBM 44826	AA 23252		R	VIII	66.4	-9.092002	147.7379
BPBM 44827	AA 23253		R	VIII	59.1	-9.092002	147.7379
BPBM 44828	AA 23254		R	VIII	57.3	-9.092002	147.7379
BPBM 44829	AA 23255		R	VIII	59.2	-9.092002	147.7379
BPBM 44830	AA 23257		R	VIII	60.6	-9.092002	147.7379
BPBM 44831	AA 23258		R	VIII	60.6	-9.092002	147.7379
BPBM 44832	AA 23259		R	VIII	56.9	-9.092002	147.7379
BPBM 44834	AA 23261		R	VIII	59.7	-9.092002	147.7379
BPBM 44835	AA 23262		R	VIII	63.4	-9.092002	147.7379
BPBM 44836	AA 23294		R	VIII	61.9	-9.10536	147.73794

BPBM 44838	AA 23296		R	VIII	65.5	-9.112397	147.726369
BPBM 44839	AA 23297		R	VIII	59.4	-9.218797	147.726369
BPBM 44840	AA 23298		R	VIII	63.9	-9.218797	147.726369
BPBM 44841	AA 23340	44841	R	VIII	63.6	-9.218797	147.726369
BPBM 44845	AA 23347		R	VIII	59.4	-9.218797	147.726369
BPBM 44846	AA 23348		R	VIII	56.9	-9.218797	147.726369
BPBM 44847	AA 23349		R	VIII	45.9	-9.218797	147.726369
BPBM 44848	AA 23350		R	VIII	62.5	-9.218797	147.726369
BPBM 44849	AA 23351		R	VIII	57.9	-9.218797	147.726369
BPBM 44853	AA 23355		R	VIII	59.7	-9.218797	147.726369
BPBM 44854	AA 23356		R	VIII	57.5	-9.218797	147.726369
BPBM 44857	AA 23390	44857	R	VIII	64.8	-9.150945	147.767477
BPBM 44860	AA 23397		R	VIII	47.7	-9.150945	147.767477
BPBM 44861	AA 23427		R	VIII	60.8	-9.118136	147.734361
BPBM 44863	AA 23437		R	VIII	64.6	-9.218797	147.726369
BPBM 44864	AA 23439		R	VIII	60.8	-9.14217	147.72617
BPBM 44865	AA 23443		R	VIII	59.8	-9.150646	147.767192
BPBM 44866	AA 23453		R	VIII	62.1	-9.150793	147.768331
BPBM 44867	AA 23454		R	VIII	59.7	-9.150793	147.768331
BPBM 44868	AA 23455		R	VIII	60.0	-9.150793	147.768331
BPBM 44869	AA 23458		R	VIII	51.2	-9.128795	147.726369
BPBM 44871	AA 23460		R	VIII	56.5	-9.14068	147.74244
BPBM 44872	AA 23475		R	VIII	58.9	-9.178219	147.767188
BPBM 44873	AA 23476		R	VIII	67.3	-9.178219	147.767188
BPBM 44874	AA 23482		R	VIII	55.5	-9.218797	147.726369
BPBM 44875	AA 23487		R	VIII	67.3	-9.11242	147.73806
BPBM 44876	AA 23488		R	VIII	64.3	-9.11242	147.73806
BPBM 44877	AA 23489		R	VIII	61.9	-9.11242	147.73806
BPBM 44878	AA 23490		R	VIII	47.7	-9.11242	147.73806

BPBM 44879	AA 23491		R	VIII	67.8	-9.11242	147.73806
BPBM 44880	AA 23492		R	VIII	62.0	-9.11242	147.73806
BPBM 44306	AA 22424	13587	S	IX	59.6	-8.20692	146.78476
BPBM 10935			T	IX	62.3	-8.576	147.072
BPBM 10936			T	IX	62.3	-8.576	147.072
BPBM 10937			T	IX	58.1	-8.576	147.072
BPBM 10938			T	IX	58.5	-8.576	147.072
BPBM 10939			T	IX	61.4	-8.576	147.072
BPBM 10940			T	IX	59.5	-8.576	147.072
BPBM 10941			T	IX	60.2	-8.576	147.072
BPBM 10942			T	IX	61.3	-8.576	147.072
BPBM 10943			T	IX	65.6	-8.576	147.072
BPBM 10944			T	IX	64.8	-8.576	147.072
BPBM 10945			T	IX	48.5	-8.576	147.072
BPBM 10946			T	IX	43.2	-8.576	147.072
BPBM 10947			T	IX	64.9	-8.576	147.072
BPBM 10948			T	IX	53.7	-8.576	147.072
BPBM 18858	FK 7896	7662	T	IX	60.9	-8.5377666	147.2423166
BPBM 18859	FK 7897	7663	T	IX	57.1	-8.5377666	147.2423166
BPBM 18861	FK 7928	7677	T	IX	62.2	-8.5448369	147.2504528
BPBM 18862	FK 7929	7678	T	IX	57.4	-8.5448369	147.2504528
BPBM 18863	FK 7939		T	IX	60.6	-8.5448369	147.2504528
BPBM 18864	FK 7940		T	IX	56.6	-8.5448369	147.2504528
BPBM 18865	FK 7941		T	IX	61.1	-8.5448369	147.2504528
BPBM 18866	FK 7959		T	IX	63.1	-8.45538	147.26301
BPBM 18867	FK 7960		T	IX	65.2	-8.45538	147.26301
BPBM 18868	FK 7961		T	IX	54.6	-8.5448369	147.2504528
BPBM 18869	FK 7962		T	IX	61.2	-8.5448369	147.2504528
BPBM 18870	FK 7963		T	IX	65.6	-8.5448369	147.2504528
BPBM 18871	FK 7964		T	IX	64.3	-8.5448369	147.2504528

BPBM 18872	FK 7965		T	IX	63.5	-8.5448369	147.2504528
BPBM 18875	FK 8039	7722	T	IX	62.4	-8.56933	147.07675
BPBM 18876	FK 8040	7723	T	IX	57.4	-8.56933	147.07675
BPBM 18877	FK 8041		T	IX	61.6	-8.56789	147.07777
BPBM 18881	FK 8056	7732	T	IX	58.2	-8.56825	147.08509
BPBM 18882	FK 8057		T	IX	58.9	-8.5668056	147.0861111
BPBM 18883	FK 8059		T	IX	56.0	-8.5668056	147.0861111

716

Table S3. Pairwise uncorrected mitochondrial sequence divergence (*p*-distances) between and within lineages of *Papuascincus* as delimited by BP&P analyses (I-IX) for the three mitochondrial gene markers (*12S*, *ND2* and *ND4*). The lower diagonal cells are *p*-distances and the upper diagonal cells are the corresponding SE values.

	I	**II**	**III**	**IV**	**V**	**VI**	**VII**	**VIII**	**IX**	**Within Lineage p-distance**	**Within Lineage SE**
12S											
I		1.0	0.8	1.1	1.1	0.9	0.9	0.9	1.0	1.94	0.49
II	5.2		1.1	1.2	1.3	1.2	1.1	1.2	1.2	0.54	0.30
III	3.9	5.9		1.1	1.1	1.0	0.9	0.9	1.0	1.77	0.44
IV	7.2	7.3	7.3		0.8	1.0	1.1	1.0	1.1	2.39	0.61
V	6.1	7.7	6.4	4.2		1.0	1.1	1.0	1.1	0.00	0.00
VI	4.5	7.0	5.2	6.0	5.1		0.8	0.8	0.9	0.58	0.23
VII	4.7	6.5	4.9	6.7	5.6	3.2		0.9	1.0	0.79	0.27
VIII	4.2	6.6	4.3	5.4	4.2	3.0	3.7		0.8	0.00	0.00
IX	5.3	7.1	5.3	6.0	4.8	3.8	4.6	3.2		0.06	0.06
ND2											
I		1.0	0.9	1.0	1.0	0.9	1.0	1.0	0.9	1.94	0.49
II	14.6		0.9	1.0	1.1	1.0	1.1	1.0	1.0	0.54	0.30
III	14.6	12.8		0.9	1.0	1.0	1.0	1.0	1.0	1.77	0.44
IV	15.9	15.3	14.5		0.9	0.9	0.9	0.9	1.0	2.39	0.61
V	15.3	15.8	15.1	11.1		1.0	1.0	1.0	1.1	0.00	0.00
VI	16.0	15.3	15.0	15.2	14.2		0.9	0.9	1.0	0.58	0.23
VII	16.0	14.9	15.6	14.6	14.1	12.4		0.9	0.9	0.79	0.27
VIII	15.2	14.8	14.6	13.6	13.1	12.8	10.6		0.9	0.00	0.00
IX	14.5	15.1	15.2	14.6	14.5	12.2	12.1	9.4		0.06	0.06
ND4											
I		1.2	1.1	1.1	1.2	1.1	1.1	1.3	1.3	5.90	0.54
II	15.1		1.0	1.2	1.3	1.3	1.3	1.3	1.4	2.28	0.47

III	14.4	11.9		1.0	1.1	1.1	1.1	1.2	1.2	6.14	0.59
IV	15.2	15.7	13.9		1.0	1.1	1.2	1.2	1.2	5.00	0.59
V	15.9	16.1	14.4	11.3		1.2	1.2	1.3	1.3	0.09	0.06
VI	14.8	14.3	14.1	13.4	14.4		1.1	1.2	1.1	1.95	0.33
VII	14.7	15.8	13.9	14.7	14.3	12.2		1.1	1.2	2.89	0.37
VIII	15.6	14.8	14.1	14.0	13.9	12.5	11.7		1.1	0.00	0.00
IX	15.7	14.9	14.1	14.7	15.1	11.6	12.4	9.7		1.29	0.24

721
722

Table S4. Pairwise uncorrected mitochondrial sequence divergence (*p*-distances) between and within lineages of *Papuascincus* as delimited by GMYC and bGMYC analyses (A-T) for the three mitochondrial gene markers (*12S*, *ND2* and *ND4*). The lower diagonal cells are *p*-distances and the upper diagonal cells are the corresponding SE values.

	A	B	C	D	E	F	G	H	I	J	K	L	M	N	O	P	Q	R	S	T	Within Lineage p-distance	Within Lineage SE
12S																						
A		1.1%	1.4%	1.5%	1.2%	1.2%	1.2%	1.2%	1.6%	1.6%	1.5%	1.4%	1.2%	1.1%	1.2%	1.2%	1.2%	1.1%	1.3%	1.2%	0.00%	0.00%
B	4.5%		1.0%	1.1%	1.0%	0.8%	0.9%	0.9%	1.2%	1.2%	1.2%	1.1%	1.1%	1.0%	1.1%	1.0%	1.0%	1.0%	1.1%	1.0%	0.00%	0.00%
C	6.8%	4.2%		0.4%	1.2%	1.1%	1.2%	1.2%	1.3%	1.3%	1.3%	1.3%	1.3%	1.2%	1.3%	1.2%	1.2%	1.2%	1.2%	1.2%	-	-
D	7.4%	4.6%	0.8%		1.3%	1.2%	1.2%	1.2%	1.3%	1.3%	1.4%	1.3%	1.3%	1.3%	1.3%	1.2%	1.2%	1.2%	1.3%	1.3%	0.00%	0.00%
E	5.8%	4.2%	6.3%	6.8%		0.8%	0.9%	0.8%	1.4%	1.4%	1.4%	1.3%	1.2%	1.2%	1.2%	1.1%	1.1%	1.1%	1.1%	1.1%	0.00%	0.00%
F	5.3%	2.5%	5.1%	5.5%	2.7%		0.7%	0.7%	1.2%	1.2%	1.2%	1.1%	1.1%	1.0%	1.1%	1.0%	1.0%	0.9%	1.1%	1.0%	0.18%	0.17%
G	5.5%	3.7%	5.5%	6.0%	3.4%	2.5%		0.6%	1.4%	1.3%	1.4%	1.3%	1.2%	1.1%	1.1%	1.0%	1.0%	1.1%	1.1%	1.1%	0.00%	0.00%
H	5.2%	3.7%	5.6%	6.0%	2.7%	1.9%	1.6%		1.3%	1.3%	1.3%	1.2%	1.1%	1.1%	1.1%	1.0%	1.0%	1.0%	1.1%	1.1%	0.00%	0.00%
I	9.3%	7.1%	7.7%	7.5%	8.5%	6.7%	8.4%	8.0%		0.5%	0.9%	1.0%	1.3%	1.2%	1.2%	1.2%	1.2%	1.2%	1.2%	1.2%	-	-
J	8.8%	6.6%	7.2%	7.2%	7.9%	6.1%	7.9%	7.4%	1.2%		1.0%	0.9%	1.3%	1.2%	1.2%	1.2%	1.2%	1.1%	1.1%	1.1%	0.26%	0.26%
K	8.7%	6.4%	7.1%	7.5%	7.7%	6.0%	7.8%	7.4%	3.6%	3.7%		1.0%	1.2%	1.1%	1.3%	1.2%	1.2%	1.1%	1.2%	1.2%	0.17%	0.12%
L	7.1%	5.8%	7.4%	7.9%	7.4%	5.4%	6.8%	6.4%	4.5%	3.8%	4.3%		1.2%	1.0%	1.2%	1.1%	1.1%	1.0%	1.1%	1.1%	0.00%	0.00%
M	5.0%	4.9%	7.2%	7.6%	6.7%	5.3%	5.9%	5.5%	7.3%	7.3%	6.5%	5.9%		0.5%	1.0%	0.9%	0.9%	0.9%	1.1%	1.0%	0.26%	0.25%
N	4.4%	4.3%	6.6%	6.9%	6.1%	4.7%	5.3%	4.8%	6.1%	6.1%	5.3%	4.8%	1.2%		0.9%	0.8%	0.8%	0.8%	0.9%	0.9%	0.09%	0.08%
O	5.2%	5.5%	6.8%	7.0%	6.6%	5.6%	5.0%	5.0%	7.1%	7.0%	7.1%	5.8%	4.1%	3.5%		0.6%	0.6%	1.0%	1.1%	1.0%	-	-
P	5.4%	4.7%	6.6%	6.8%	6.1%	5.2%	4.5%	4.8%	7.2%	6.9%	6.5%	5.8%	3.8%	3.2%	1.5%		0.4%	0.9%	1.0%	1.0%	0.70%	0.33%
Q	5.0%	4.3%	6.1%	6.3%	5.8%	4.9%	4.3%	4.3%	6.9%	6.6%	6.3%	5.3%	3.4%	2.7%	1.4%	0.8%		0.8%	1.0%	1.0%	0.13%	0.12%
R	4.2%	4.2%	6.3%	6.8%	5.0%	3.8%	4.7%	4.2%	6.1%	5.5%	5.1%	4.2%	3.8%	2.7%	4.2%	3.9%	3.5%		0.8%	0.8%	0.00%	0.00%
S	5.8%	5.5%	6.6%	7.0%	6.3%	5.4%	5.8%	5.3%	6.3%	5.8%	6.0%	5.0%	4.9%	3.7%	5.2%	5.0%	4.5%	3.4%		0.2%	-	-
T	5.5%	5.2%	6.8%	7.3%	6.0%	5.1%	5.5%	5.0%	6.3%	5.8%	6.0%	4.7%	4.6%	3.5%	5.0%	4.7%	4.3%	3.1%	0.3%		0.00%	0.00%
ND2																						
A		0.93%	1.05%	1.10%	1.11%	1.06%	1.06%	1.09%	1.09%	1.08%	1.09%	1.08%	1.10%	1.11%	1.13%	1.06%	1.10%	1.08%	1.03%	1.08%	0.29%	0.17%
B	11.86%		1.05%	1.15%	1.07%	1.06%	1.07%	1.15%	1.10%	1.08%	1.09%	1.11%	1.01%	1.05%	1.10%	1.08%	1.14%	1.04%	0.95%	0.96%	0.34%	0.12%
C	14.12%	13.90%		0.59%	1.00%	1.04%	1.02%	1.05%	1.04%	1.06%	1.07%	1.11%	1.07%	1.05%	1.07%	1.07%	1.08%	1.06%	1.05%	1.06%	-	-
D	14.71%	15.02%	3.35%		1.05%	1.06%	1.09%	1.04%	1.07%	1.07%	1.11%	1.11%	1.14%	1.11%	1.09%	1.12%	1.14%	1.11%	1.11%	1.09%	0.22%	0.15%

E	15.29%	13.19%	11.57%	12.47%		0.87%	0.84%	0.91%	1.06%	1.07%	1.06%	1.08%	1.13%	1.07%	1.06%	1.10%	1.07%	1.03%	1.09%	1.06%	0.00%	0.00%
F	15.46%	14.26%	13.50%	12.99%	8.69%		0.84%	0.83%	1.08%	1.08%	1.08%	1.04%	1.05%	1.02%	1.08%	1.04%	1.05%	1.09%	1.06%	1.00%	0.13%	0.09%
G	15.05%	14.36%	12.84%	13.23%	9.71%	8.55%		0.61%	1.07%	1.07%	1.08%	1.10%	1.09%	1.02%	1.12%	1.08%	1.07%	1.06%	1.06%	1.05%	0.49%	0.22%
H	15.14%	14.87%	12.43%	12.82%	9.26%	8.52%	4.49%		1.15%	1.17%	1.16%	1.10%	1.09%	1.09%	1.15%	1.12%	1.14%	1.09%	1.12%	1.13%	0.56%	0.17%
I	16.52%	15.40%	14.61%	15.45%	14.41%	14.41%	14.07%	13.72%		0.40%	0.83%	0.95%	1.13%	1.10%	1.04%	1.09%	1.10%	1.00%	0.99%	1.03%	-	-
J	16.62%	15.84%	15.10%	15.97%	14.71%	14.74%	14.31%	14.48%	1.76%		0.84%	0.94%	1.10%	1.08%	1.03%	1.06%	1.06%	0.99%	1.00%	1.03%	0.20%	0.14%
K	16.13%	15.90%	14.80%	15.35%	14.31%	14.77%	14.56%	14.68%	8.33%	8.92%		0.96%	1.15%	1.10%	1.06%	1.08%	1.09%	1.01%	1.10%	1.07%	0.00%	0.00%
L	14.59%	15.55%	15.60%	15.97%	15.59%	15.09%	15.40%	14.87%	11.09%	11.20%	10.98%		1.07%	1.05%	1.10%	1.04%	1.10%	0.99%	1.09%	1.11%	0.00%	0.00%
M	16.29%	15.72%	14.95%	15.85%	14.73%	14.18%	15.00%	15.53%	14.25%	14.57%	15.27%	14.62%		0.60%	0.99%	1.00%	1.00%	0.98%	1.00%	0.99%	0.54%	0.23%
N	16.62%	15.94%	14.90%	15.38%	14.68%	14.50%	14.95%	15.44%	14.55%	15.01%	15.89%	14.05%	4.64%		0.94%	1.01%	1.03%	1.00%	0.96%	0.97%	0.14%	0.07%
O	16.13%	15.38%	14.61%	15.14%	14.22%	15.26%	15.64%	15.13%	13.92%	13.82%	13.82%	13.69%	11.94%	11.62%		0.73%	0.76%	0.95%	0.95%	0.95%	-	-
P	15.13%	15.40%	13.97%	14.70%	14.17%	15.09%	15.48%	15.23%	14.45%	14.31%	14.39%	13.67%	12.19%	12.16%	6.09%		0.48%	0.94%	0.95%	0.98%	0.64%	0.21%
Q	16.18%	16.67%	14.99%	15.48%	15.02%	16.13%	16.26%	16.38%	15.28%	15.05%	14.67%	14.56%	13.01%	12.77%	7.00%	2.92%		0.98%	0.94%	1.00%	0.83%	0.20%
R	15.39%	15.19%	14.26%	15.04%	13.58%	14.92%	15.59%	14.36%	14.17%	14.66%	12.79%	13.09%	12.42%	12.97%	10.64%	10.13%	11.01%		0.88%	0.89%	0.10%	0.10%
S	14.46%	13.42%	14.71%	15.55%	13.53%	14.67%	15.54%	15.54%	14.71%	15.29%	14.31%	14.30%	12.04%	12.13%	10.98%	11.09%	11.87%	9.17%		0.47%	-	-
T	15.13%	14.36%	14.70%	15.20%	14.27%	14.55%	15.51%	15.87%	14.55%	15.24%	14.15%	14.55%	12.47%	12.10%	11.42%	12.07%	12.36%	9.42%	2.75%		0.48%	0.15%
ND4																						
A		1.2%	1.4%	1.3%	1.4%	1.2%	1.4%	1.4%	1.3%	1.3%	1.3%	1.3%	1.2%	1.3%	1.3%	1.3%	1.3%	1.4%	1.4%	1.4%	0.14%	0.14%
B	13.4%		1.4%	1.3%	1.3%	1.2%	1.3%	1.4%	1.4%	1.4%	1.3%	1.3%	1.3%	1.3%	1.3%	1.3%	1.3%	1.4%	1.3%	1.4%	0.27%	0.12%
C	15.5%	15.7%		0.7%	1.2%	1.2%	1.2%	1.1%	1.2%	1.3%	1.4%	1.4%	1.4%	1.3%	1.4%	1.4%	1.4%	1.3%	1.4%	1.4%	-	-
D	15.2%	14.7%	3.4%		1.2%	1.1%	1.1%	1.1%	1.2%	1.3%	1.3%	1.4%	1.3%	1.3%	1.3%	1.4%	1.3%	1.3%	1.3%	1.4%	0.00%	0.00%
E	15.8%	14.8%	11.8%	11.8%		1.0%	1.1%	1.0%	1.2%	1.3%	1.4%	1.3%	1.3%	1.3%	1.3%	1.3%	1.3%	1.4%	1.3%	1.3%	0.00%	0.00%
F	15.2%	13.9%	12.2%	11.8%	8.3%		1.0%	1.0%	1.2%	1.2%	1.3%	1.3%	1.3%	1.3%	1.3%	1.4%	1.3%	1.3%	1.3%	1.3%	0.09%	0.09%
G	15.6%	14.3%	12.2%	12.4%	8.8%	8.4%		0.8%	1.3%	1.2%	1.3%	1.2%	1.3%	1.3%	1.3%	1.3%	1.3%	1.4%	1.3%	1.3%	0.60%	0.28%
H	15.2%	14.0%	11.8%	11.8%	8.1%	8.3%	5.8%		1.2%	1.2%	1.2%	1.3%	1.2%	1.3%	1.2%	1.3%	1.3%	1.3%	1.3%	1.3%	0.58%	0.22%
I	15.9%	15.2%	14.0%	14.4%	13.2%	13.4%	14.3%	12.0%		0.4%	1.0%	1.1%	1.2%	1.2%	1.2%	1.2%	1.3%	1.3%	1.3%	1.3%	-	-
J	15.5%	14.8%	14.2%	14.9%	14.2%	13.3%	14.2%	12.0%	1.4%		0.9%	1.1%	1.2%	1.2%	1.2%	1.3%	1.3%	1.3%	1.3%	1.3%	0.00%	0.00%
K	16.3%	15.0%	17.1%	16.8%	16.0%	14.6%	15.5%	14.1%	8.6%	7.7%		1.2%	1.3%	1.2%	1.2%	1.3%	1.3%	1.4%	1.4%	1.4%	0.10%	0.09%
L	15.6%	16.0%	16.1%	16.1%	15.6%	14.9%	14.6%	13.6%	10.6%	10.5%	12.1%		1.2%	1.3%	1.2%	1.2%	1.3%	1.3%	1.2%	1.3%	0.09%	0.06%
M	14.8%	14.9%	14.3%	14.4%	14.2%	14.3%	15.2%	13.8%	11.6%	12.4%	14.6%	13.7%		0.8%	1.1%	1.2%	1.2%	1.1%	1.2%	1.2%	0.15%	0.14%
N	14.5%	14.8%	13.9%	14.4%	14.0%	14.3%	15.4%	13.4%	12.2%	12.7%	14.4%	14.6%	4.4%		1.2%	1.3%	1.3%	1.3%	1.2%	1.2%	0.10%	0.07%
O	14.9%	14.3%	15.4%	15.3%	14.1%	14.9%	13.5%	12.8%	12.1%	12.2%	14.6%	12.8%	11.2%	12.8%		0.8%	0.9%	1.1%	1.2%	1.2%	-	-
P	15.7%	14.1%	16.0%	16.0%	13.5%	14.6%	13.5%	12.9%	13.6%	13.7%	15.7%	13.9%	11.2%	12.2%	5.8%		0.5%	1.1%	1.2%	1.2%	0.94%	0.29%
Q	15.4%	14.7%	16.0%	15.8%	13.8%	14.9%	14.4%	13.9%	14.1%	14.3%	15.8%	14.9%	11.5%	12.5%	6.7%	2.4%		1.2%	1.2%	1.2%	0.87%	0.25%

R	15.9%	15.5%	14.2%	15.1%	15.0%	13.9%	15.0%	13.4%	13.6%	13.1%	14.8%	13.9%	11.3%	12.9%	11.2%	11.5%	12.0%		1.1%	1.1%	0.00%	0.00%
S	16.3%	15.7%	14.5%	15.0%	14.2%	13.8%	15.3%	13.8%	13.1%	13.5%	16.4%	14.6%	11.7%	11.5%	11.7%	12.6%	12.6%	10.2%		0.7%	-	-
T	16.0%	15.6%	14.5%	15.1%	14.3%	14.1%	15.3%	13.7%	13.7%	13.9%	15.5%	15.1%	11.7%	11.6%	12.1%	12.3%	12.4%	9.6%	3.6%		0.63%	0.19%

726

727

Table S5. Pairwise comparisons of SVL between different GMYC/bGMYC lineages, performed using a *post-hoc* Tukey test. The upper triangle shows the adjusted p values for each pair of lineages, from the corresponding row and column. Significant p values, with an alpha of 0.05, are marked in bold. Cells shaded light grey represent comparisons between lineages of the small morph, cells shaded dark grey represent comparisons between lineages of the large morph, and unshaded cells represent comparisons between lineages of different morphs. The two right-most columns show the mean SVL (in mm) ± standard error, and the sample size for each lineage.

GMYC/bGMYC Lineage	A	B	C	D	E	F	G	H	I	J	K	L	M	N	O	P	Q	R	S	T	Mean SVL	n
A		0.851	1	0.095	**0**	1	1	0.902	0.347	**0**	**0**	1	0.915	**0**	**0.001**	0.153	**0**	**0**	0.3	**0**	49.5 ± 0.41	46
B			1	**0.001**	**0**	0.44	1	**0.03**	0.977	**0**	**0**	**0.032**	0.989	**0**	**0.013**	0.619	**0**	**0**	0.556	**0**	50.8 ± 0.28	106
C				1	0.776	1	1	1	1	0.711	0.618	1	0.979	0.051	0.584	0.972	0.473	0.207	0.693	0.1	48.1	1
D					**0.036**	0.877	0.902	0.991	**0**	**0**	**0**	0.362	0.248	**0**	**0**	**0**	**0**	**0**	**0.017**	**0**	45.6 ± 0.57	11
E						**0**	**0.001**	**0**	**0**	**0**	**0**	**0**	**0.001**	**0**	**0**	**0**	**0**	**0**	**0**	**0**	40 ± 0.62	9
F							1	1	0.111	**0**	**0**	1	0.767	**0**	**0**	**0.046**	**0**	**0**	0.16	**0**	48.4 ± 0.48	17
G								1	0.997	0.041	0.018	1	0.973	**0**	0.107	0.818	**0.009**	**0**	0.525	**0**	49.7 ± 0.99	4
H									**0.011**	**0**	**0**	0.999	0.615	**0**	**0**	**0.009**	**0**	**0**	0.089	**0**	47.7 ± 0.41	20
I										0.07	**0.019**	**0.04**	1	**0**	0.442	1	**0.014**	**0**	0.905	**0**	52.5 ± 1.2	14
J											1	**0**	1	**0**	1	1	1	0.056	1	**0.005**	56.3 ± 0.6	35
K												**0**	1	**0.003**	1	1	1	0.294	1	**0.032**	56.7 ± 0.62	35
L													0.811	**0**	**0**	**0.034**	**0**	**0**	0.182	0	48.8 ± 0.28	64
M														1	1	1	1	1	1	1	56.4	1
N															0.992	0.06	0.402	0.645	1	1	60.6 ± 0.75	24
O																0.999	1	1	1	1	57.7 ± 0.92	4
P																	0.99	0.56	0.999	0.197	54.7 ± 0.97	5
Q																		1	1	0.855	57.5 ± 1.13	15
R																			1	0.994	58.7 ± 0.51	86
S																				1	59.6	1
T																					59.8 ± 0.82	34

REFERENCES

Abbott, L.D. 1995. Neogene tectonic reconstruction of the Adelbert-Finisterre-New Britain collision, northern Papua New Guinea. J. Southeast Asian Earth Sci. 11, 33-51. https://doi.org/10.1016/0743-9547(94)00032-A.

Abbott, L.D., Silver, E.A., Thompson, P.R., Filewicz, M.V., Schneider, C., Abdoerrias. 1994. Stratigraphic constraints on the development and timing of arc-continent collision in northern Papua New Guinea. J. Sediment. Res. 64, 169-183. https://doi.org/10.1306/D4267F82-2B26-11D7-8648000102C1865D.

Allison, A. 1982. Distribution and ecology of New Guinea lizards, in: Gressit, J.L. (Ed.), Biogeography and ecology of New Guinea. Springer, The Hague, Netherlands, pp. 803-813.

Allison, A. 2009. New Guinea, Biology, in: Gillespie, R.G., Clague, D.A. (Eds.), Encyclopedia of islands. University of California Press, Berkley and Los Angeles, California, pp. 652-658.

Allison, A., Greer, A.E. 1986. Egg shells with pustulate surface structures: basis for a new genus of New Guinea skinks (Lacertilia: Scincidae). J. Herpetol. 20, 116-119. https://doi.org/10.2307/1564142.

Baldwin, S.L., Fitzgerald, P.G., Webb, L.E. 2012. Tectonics of the New Guinea Region. Annu. Rev. Earth Plan. Sci. 40, 495-520. https://doi.org/10.1146/annurev-earth-040809-152540.

Bickford, D., Lohman, D.J., Sodhi, N.S., Ng, P.K., Meier, R., Winker, K., Ingram, K.K., Das, I. 2007. Cryptic species as a window on diversity and conservation. Trends Ecol. Evol. 22, 148-155. https://doi.org/10.1016/j.tree.2006.11.004.

Boulenger, G.A. 1897. Descriptions of new lizards and frogs from Mount Victoria, Owen Stanley Range, New Guinea, collected by Mr. A. S. Anthony. Ann. Mag. Nat. Hist. Series Six. 19, 6-13. https://doi.org/10.1080/00222939708680502.

Brooks, T.M., Mittermeier, R.A., da Fonseca, G.A.B., Gerlach, J., Hoffmann, M., Lamoreux, J.F., Mittermeier, C.G., Pilgrim, J.D., Rodrigues, A.S.L. 2006. Global biodiversity conservation priorities. Science. 313, 58-61. https://doi.org/10.1126/science.1127609.

764 Brown, W.L.,Wilson, E.O. 1956. Character displacement. Syst. Zool. 5, 49-64.
765 https://doi.org/10.2307/2411924.
766 Bruen, T.C., Philippe, H., Bryant, D. 2006. A simple and robust statistical test for
767 detecting the presence of recombination. Genetics. 172, 2665-2681.
768 https://doi.org/10.1534/genetics.105.048975.
769 Bryan, J.E., Shearman, P.L. 2015. The state of the forests of Papua New Guinea 2014:
770 measuring change over the period 2002-2014. University of Papua New Guinea, Port
771 Moresby, Papua New Guinea.
772 Chazot, N., Willmott, K.R., Condamine, F.L., De-Silva, D.L., Freitas, A.V.L., Lamas, G.,
773 Morlon, H., Giraldo, C.E., Jiggins, C.D., Joron, M. 2016. Into the Andes: multiple
774 independent colonizations drive montane diversity in the Neotropical clearwing
775 butterflies *Godyridina*. Mol. Ecol. 25, 5765-5784. https://doi.org/10.1111/mec.13773.
776 Clement, M., Posada, D.C.K.A., Crandall, K.A. 2000. TCS: a computer program to
777 estimate gene genealogies. Mol. Ecol. 9, 1657-1659. https://doi.org/10.1046/j.1365-
778 294x.2000.01020.x.
779 Craft, K.J., Pauls, S.U., Darrow, K., Miller, S.E., Hebert, P.D., Helgen, L.E., Novotny, V.,
780 Weiblen, G.D. 2010. Population genetics of ecological communities with DNA barcodes:
781 An example from New Guinea Lepidoptera. Proc. Natl. Acad. Sci. USA. 107, 5041-5046.
782 https://doi.org/10.1073/pnas.0913084107.
783 Davies, T.J., Meiri, S., Barraclough, T.G., Gittleman, J.L. 2007. Species co-existence
784 and character divergence across carnivores. Ecol. Lett. 10, 146-152.
785 https://doi.org/10.1111/j.1461-0248.2006.01005.x.
786 Dayan, T., Simberloff, D. 2005. Ecological and community-wide character
787 displacement: the next generation. Ecol. Lett. 8, 875-894.
788 https://doi.org/10.1111/j.1461-0248.2005.00791.x.
789 Diamond, J.M. 1973. Distributional ecology of New Guinea birds. Science. 179, 759-
790 769. https://doi.org/10.1126/science.179.4075.759.
791 Donnellan, S.C., Aplin, K.P. 1989. Resolution of cryptic species in the New Guinean
792 lizard, *Sphenomorphus jobiensis* (Scincidae) by electrophoresis. Copeia. 1989, 81-88.
793 https://doi.org/10.2307/1445608.

794 Drummond, A.J., Suchard, M.A., Xie, D., Rambaut, A. 2012. Bayesian phylogenetics
795 with BEAUti and the BEAST 1.7. Mol. Biol. Evol. 29, 1969-1973.
796 https://doi.org/10.1093/molbev/mss075.
797 Elias, M., Joron, M., Willmott, K., Silva-Brandão, K.L., Kaiser, V., Arias, C.F., Piñerez,
798 L.M.G., Uribe, S., Brower, A.V.Z., Freitas, A.V.L. 2009. Out of the Andes: patterns of
799 diversification in clearwing butterflies. Mol. Ecol. 18, 1716-1729.
800 https://doi.org/10.1111/j.1365-294X.2009.04149.x.
801 Ezard, T., Fujisawa, T., Barraclough, T.G. 2009. splits: SPecies' LImits by Threshold
802 Statistics. R package version 1.0-19. https://rdrr.io/rforge/splits/.
803 Flot, J.F. 2010. SeqPHASE: a web tool for interconverting PHASE input/output files
804 and FASTA sequence alignments. Mol. Ecol. Resour. 10, 162-166.
805 https://doi.org/10.1111/j.1755-0998.2009.02732.x.
806 Fritz, S.A., Jønsson, K.A., Fjeldså, J., Rahbek, C. 2012. Diversification and
807 biogeographic patterns in four island radiations of passerine birds. Evolution. 66, 179-
808 190. https://doi.org/10.1111/j.1558-5646.2011.01430.x.
809 Georges, A., Zhang, X., Unmack, P., Reid, B.N., Le, M., McCord, W.P. 2013.
810 Contemporary genetic structure of an endemic freshwater turtle reflects Miocene
811 orogenesis of New Guinea. Biol. J. Linn. Soc. 111, 192-208.
812 https://doi.org/10.1111/bij.12176
813 Givnish, T.J., Spalink, D., Ames, M., Lyon, S.P., Hunter, S.J., Zuluaga, A., Iles, W.J.,
814 Clements, M.A., Arroyo, M.T., Leebens-Mack, J. 2015. Orchid phylogenomics and
815 multiple drivers of their extraordinary diversification. Proc. Roy. Soc. B. Biol. Sci. 282,
816 20151553. https://doi.org/10.1098/rspb.2015.1553.
817 Grant, P.R. 1972. Convergent and divergent character displacement. Biol. J. Linn. Soc.
818 4, 39-68. https://doi.org/10.1111/j.1095-8312.1972.tb00690.x.
819 Grant, P.R., Grant, B.R. 2006. Evolution of character displacement in Darwin's
820 finches. Science. 313, 224-226. https://doi.org/10.1126/science.1128374.
821 Greer, A.E. 1974. The generic relationships of the scincid lizard genus *Leiolopisma*
822 and its relatives. Aust. J. Zool. Supp. Ser. 22, 1-67. https://doi.org/10.1071/AJZS031.
823 Greer, A.E., Allison, A., Cogger, H.G. 2005. Four new species of *Lobulia* (Lacertilia:
824 Scincidae) from high altitude in New Guinea. Herpetol. Monogr. 19, 153-179.
825 https://doi.org/10.1655/0733-1347(2005)019[0153:FNSOLL]2.0.CO;2.

826 Hall, R. 2002. Cenozoic geological and plate tectonic evolution of SE Asia and the SW
827 Pacific: computer-based reconstructions, model and animations. J. Asian Earth Sci. 20,
828 353-431. https://doi.org/10.1016/S1367-9120(01)00069-4.
829 Hill, K.C., Raza, A. 1999. Arc-continent collision in Papua Guinea: Constraints from
830 fission track thermochronology. Tectonics. 18, 950-966.
831 https://doi.org/10.1029/1999TC900043.
832 Hill, K.C., Hall, R. 2003. Mesozoic-Cenozoic evolution of Australia's New Guinea
833 margin in a west Pacific context. Geol. Soc. Amer. Spec. Pap. 372, 265-290.
834 https://doi.org/10.1130/0-8137-2372-8.265.
835 Hillis, D.M. 2019. Species delimitation in herpetology. J. Herpetol. 53, 3-12.
836 https://doi.org/10.1670/18-123.
837 Hope, G., Golson, J. 1995. Late Quaternary change in the mountains of New Guinea.
838 Antiquity. 69, 818-830. https://doi.org/10.1017/S0003598X00082363.
839 Huson, D.H., Bryant, D. 2006. Application of phylogenetic networks in evolutionary
840 studies. Mol. Biol. Evol. 23, 254-267. https://doi.org/10.1093/molbev/msj030.
841 Hutter, C.R., Guayasamin, J.M., Wiens, J.J. 2013. Explaining Andean megadiversity:
842 the evolutionary and ecological causes of glassfrog elevational richness patterns. Ecol.
843 Lett. 16, 1135-1144. https://doi.org/10.1111/ele.12148.
844 Jackson, N.D., Carstens, B.C., Morales, A.E., O'Meara, B.C. 2017. Species delimitation
845 with gene flow. Syst. Biol. 66, 799-812. https://doi.org/10.1093/sysbio/syw117.
846 Jörger, K.M., Schrödl, M. 2013. How to describe a cryptic species? Practical
847 challenges of molecular taxonomy. Front. Zool. 10, 59. https://doi.org/10.1186/1742-
848 9994-10-59.
849 Kadarusman, Hubert, N., Hadiaty, R.K., Sudarto, Paradis, E., Pouyaud, L. 2012.
850 Cryptic diversity in Indo-Australian rainbowfishes revealed by DNA barcoding:
851 implications for conservation in a biodiversity hotspot candidate. PLoS One. 7, e40627.
852 https://doi.org/10.1371/journal.pone.0040627.
853 Katoh, K., Standley, D.M. 2013. MAFFT multiple sequence alignment software
854 version 7: improvements in performance and usability. Mol. Biol. Evol. 30, 772-780.
855 https://doi.org/10.1093/molbev/mst010.

856 Kumar, S., Stecher, G., Tamura, K. 2016. MEGA7: molecular evolutionary genetics
857 analysis version 7.0 for bigger datasets. Mol. Biol. Evol. 33, 1870-1874.
858 https://doi.org/10.1093/molbev/msw054.
859 Lanfear, R., Frandsen, P.B., Wright, A.M., Senfeld, T., Calcott, B. 2016.
860 PartitionFinder 2: new methods for selecting partitioned models of evolution for
861 molecular and morphological phylogenetic analyses. Mol. Biol. Evol. 34, 772-773.
862 https://doi.org/10.1093/molbev/msw260.
863 Leaché, A.D., Zhu, T., Rannala, B., Yang, Z. 2019. The spectre of too many species.
864 Syst. Biol. 68, 168-181. https://doi.org/10.1093/sysbio/syy051.
865 Leigh, J.W., Bryant, D. 2015. popart: full-feature software for haplotype network
866 construction. Methods Ecol. Evol. 6, 1110-1116. https://doi.org/10.1111/2041-
867 210X.12410.
868 Lemey, P., Rambaut, A., Drummond, A.J., Suchard, M.A. 2009. Bayesian
869 phylogeography finds its roots. PLoS Comput. Biol. 5, e1000520.
870 https://doi.org/10.1371/journal.pcbi.1000520.
871 Linkem, C.W., Diesmos, A.C., Brown, R.M. 2011. Molecular systematics of the
872 Philippine forest skinks (Squamata: Scincidae: *Sphenomorphus*): testing morphological
873 hypotheses of interspecific relationships. Zool. J. Linn. Soc. 163, 1217-1243.
874 https://doi.org/10.1111/j.1096-3642.2011.00747.x.
875 Losos, J.B. 2008. Phylogenetic niche conservatism, phylogenetic signal and the
876 relationship between phylogenetic relatedness and ecological similarity among species.
877 Ecol. Lett. 11, 995-1003. https://doi.org/10.1111/j.1461-0248.2008.01229.x.
878 Marki, P.Z., Jønsson, K.A., Irestedt, M., Nguyen, J.M.T., Rahbek, C., Fjeldså, J. 2017.
879 Supermatrix phylogeny and biogeography of the Australasian Meliphagides radiation
880 (Aves: Passeriformes). Mol. Phylogenet. Evol. 107, 516-529.
881 https://doi.org/10.1016/j.ympev.2016.12.021.
882 Mayr, E., Diamond, J.M. 1976. Birds on islands in the sky: origin of the montane
883 avifauna of northern Melanesia. Proc. Natl. Acad. Sci. USA. 73, 1765-1769.
884 https://doi.org/10.1073/pnas.73.5.1765.
885 McGuigan, K., Zhu, D., Allen, G.R., Moritz, C. 2000. Phylogenetic relationships and
886 historical biogeography of melanotaeniid fishes in Australia and New Guinea. Mar.
887 Freshwater Res. 51, 713-723. https://doi.org/10.1071/MF99159.

888 Meiri, S., Brown, J.H., Sibly, R.M. 2012. The ecology of lizard reproductive output.
889 Global Ecol. Biogeogr. 21, 592-602. https://doi.org/10.1111/j.1466-8238.2011.00700.x.
890 Meiri, S., Bauer, A.M., Allison, A., Castro-Herrera, F., Chirio, L., Colli, G., Das, I., Doan,
891 T.M., Glaw, F., Grismer, L.L., Hoogmoed, M., Kraus, F., LeBreton, M., Meirte, D., Nagy,
892 Z.T., Nogueira, C.d.C., Oliver, P., Pauwels, O.S.G., Pincheira-Donoso, D., Shea, G.,
893 Sindaco, R., Tallowin, O.J.S., Torres-Caravajal, O., Trape, J.-F., Uetz, P., Wagner, P., Wang,
894 Y., Ziegler, T., Roll, U. 2018. Extinct, obscure or imaginary: The lizard species with the
895 smallest ranges. Divers. Distrib. 24, 262-273. https://doi.org/10.1111/ddi.12678.
896 Metzger, G.A., Kraus, F., Allison, A., Parkinson, C.L. 2010. Uncovering cryptic
897 diversity in *Aspidomorphus* (Serpentes: Elapidae): evidence from mitochondrial and
898 nuclear markers. Mol. Phylogenet. Evol. 54, 405-416.
899 https://doi.org/10.1016/j.ympev.2009.07.027.
900 Myers, N., Mittermeier, R.A., Mittermeier, C.G., Da Fonseca, G.A., Kent, J. 2000.
901 Biodiversity hotspots for conservation priorities. Nature. 403, 853-858.
902 https://doi.org/10.1038/35002501.
903 Olave, M., Solà, E., Knowles, L.L. 2014. Upstream analyses create problems with
904 DNA-based species delimitation. Syst. Biol. 63, 263-271.
905 https://doi.org/10.1093/sysbio/syt106.
906 Oliver, L.A., Rittmeyer, E.N., Kraus, F., Richards, S.J., Austin, C.C. 2013. Phylogeny
907 and phylogeography of *Mantophryne* (Anura: Microhylidae) reveals cryptic diversity in
908 New Guinea. Mol. Phylogenet. Evol. 67, 600-607.
909 https://doi.org/10.1016/j.ympev.2013.02.023.
910 Oliver, P.M., Iannella, A., Richards, S.J., Lee, M.S.Y. 2017. Mountain colonisation,
911 miniaturisation and ecological evolution in a radiation of direct-developing New Guinea
912 Frogs (*Choerophryne*, Microhylidae). PeerJ, 5, e3077.
913 https://doi.org/10.7717/peerj.3077.
914 Pante, E., Puillandre, N., Viricel, A., Arnaud-Haond, S., Aurelle, D., Castelin, M.,
915 Chenuil, A., Destombe, C., Forcioli, D., Valero, M. 2015. Species are hypotheses: avoid
916 connectivity assessments based on pillars of sand. Mol. Ecol. 24, 525-544.
917 https://doi.org/10.1111/mec.13048.

Parker, H.W. 1936. A collection of reptiles and amphibians from the mountains of British New Guinea. Ann. Mag. Nat. Hist. Series 10. 17, 66-93. https://doi.org/10.1080/03745481.1936.10801389.

Pigram, C.J., Davies, H.L. 1987. Terranes and the accretion history of the New Guinea orogen. BMR J. Aust. Geol. Geophys. 10, 193-211.

Pons, J., Barraclough, T.G., Gomez-Zurita, J., Cardoso, A., Duran, D.P., Hazell, S., Kamoun, S., Sumlin, W.D., Vogler, A.P. 2006. Sequence-based species delimitation for the DNA taxonomy of undescribed insects. Syst. Biol. 55, 595-609. https://doi.org/10.1080/10635150600852011.

Porter, S.C. 2000. Snowline depression in the tropics during the Last Glaciation. Quaternary Sci. Rev. 20, 1067-1091. https://doi.org/10.1016/S0277-3791(00)00178-5.

Quarles van Ufford, A., Cloos, M. 2005. Cenozoic tectonics of New Guinea. AAPG Bull. 89, 119-140. https://doi.org/10.1306/08300403073.

R Core Team 2017. R: A language and environment for statistical computing. R Foundation for Statistical Computing, Vienna, Austria.

Rabosky, D.L., Donnellan, S.C., Talaba, A.L., Lovette, I.J. 2007. Exceptional among-lineage variation in diversification rates during the radiation of Australia's most diverse vertebrate clade. Proc. Roy. Soc. B. Biol. Sci. 274, 2915-2923. https://doi.org/10.1098/rspb.2007.0924.

Rabosky, D.L., Donnellan, S.C., Grundler, M., Lovette, I.J. 2014. Analysis and visualization of complex macroevolutionary dynamics: an example from Australian scincid lizards. Syst. Biol. 63, 610-627. https://doi.org/10.1093/sysbio/syu025.

Rambaut, A., Suchard, M.A., Xie, D., Drummond, A.J. 2014. Tracer v1.6. http://beast.bio.ed.ac.uk/Tracer.

Rannala, B., Yang, Z. 2003. Bayes estimation of species divergence times and ancestral population sizes using DNA sequences from multiple loci. Genetics. 164, 1645-1656.

Rannala, B., Yang, Z. 2013. Improved reversible jump algorithms for Bayesian species delimitation. Genetics. 194, 245-253. https://doi.org/10.1534/genetics.112.149039.

Rawlings, L.H., Donnellan, S.C. 2003. Phylogeographic analysis of the green python, *Morelia viridis*, reveals cryptic diversity. Mol. Phylogenet. Evol. 27, 36-44. https://doi.org/10.1016/S1055-7903(02)00396-2.

Reid, N.M., Carstens, B.C. 2012. Phylogenetic estimation error can decrease the accuracy of species delimitation: a Bayesian implementation of the general mixed Yule-coalescent model. BMC Evol. Biol. 12, 196. https://doi.org/10.1186/1471-2148-12-196.

Revell, L.J. 2012. phytools: An R package for phylogenetic comparative biology (and other things). Methods Ecol. Evol. 3, 217-223. https://doi.org/10.1111/j.2041-210X.2011.00169.x.

Rodriguez, Z.B., Perkins, S.L., Austin, C.C. 2018 Multiple origins of green blood in New Guinea lizards. Sci. Advances. 4, eaao5017. https://doi.org/10.1126/sciadv.aao5017.

Ronquist, F., Teslenko, M., Van Der Mark, P., Ayres, D.L., Darling, A., Höhna, S., Larget, B., Liu, L., Suchard, M.A., Huelsenbeck, J.P. 2012. MrBayes 3.2: efficient Bayesian phylogenetic inference and model choice across a large model space. Syst. Biol. 61, 539-542. https://doi.org/10.1093/sysbio/sys029.

Santos, J.C., Coloma, L.A., Summers, K., Caldwell, J.P., Ree, R., Cannatella, D.C. 2009. Amazonian amphibian diversity is primarily derived from late Miocene Andean lineages. PLoS Biol. 7, e1000056. https://doi.org/10.1371/journal.pbio.1000056.

Sauer, C.O. 1915. Exploration of the Kaiserin Augusta River in New Guinea, 1912-13. Bull. Amer. Geogr. Soc. 47, 342-345. https://doi.org/10.2307/201196.

Schenk, J.J. 2016. Consequences of secondary calibrations on divergence time estimates. PLoS One. 11, e0148228. https://doi.org/10.1371/journal.pone.0148228.

Sedano, R.E., Burns, K.J. 2010. Are the Northern Andes a species pump for Neotropical birds? Phylogenetics and biogeography of a clade of Neotropical tanagers (Aves: Thraupini). J. Biogeogr. 37, 325-343. https://doi.org/10.1111/j.1365-2699.2009.02200.x.

Silvestro, D., Michalak, I. 2012. raxmlGUI: a graphical front-end for RAxML. Org. Divers. Evol. 12, 335-337. https://doi.org/10.1007/s13127-011-0056-0.

Simberloff, D., Dayan, T., Jones, C., Ogura, G. 2000. Character displacement and release in the small Indian mongoose, *Herpestes javanicus*. Ecology. 81, 2086-2099. https://doi.org/10.1890/0012-9658(2000)081[2086:CDARIT]2.0.CO;2.

Skinner, A., Hugall, A.F., Hutchinson, M.N. 2011. Lygosomine phylogeny and the origins of Australian scincid lizards. J. Biogeogr. 38, 1044-1058. https://doi.org/10.1111/j.1365-2699.2010.02471.x.

Slatkin, M. 1980. Ecological character displacement. Ecology. 61, 163-177. https://doi.org/10.2307/1937166.

Stephens, M., Scheet, P. 2005. Accounting for decay of linkage disequilibrium in haplotype inference and missing-data imputation. Amer. J. Hum. Genet. 76, 449-462. https://doi.org/10.1086/428594.

Stephens, M., Smith, N.J., Donnelly, P. 2001. A new statistical method for haplotype reconstruction from population data. Amer. J. Hum. Genet. 68, 978-989. https://doi.org/10.1086/319501.

Sukumaran, J., Knowles, L.L. 2017. Multispecies coalescent delimits structure, not species. Proc. Natl. Acad. Sci. USA. 114, 1607-1612. https://doi.org/10.1073/pnas.1607921114.

Tallowin, O.J.S., Allison, A., Algar, A.C., Kraus, F., Meiri, S. 2017. Papua New Guinea terrestrial-vertebrate richness: elevation matters most for all except reptiles. J. Biogeogr. 44, 1734-1744. https://doi.org/10.1111/jbi.12949.

Tallowin, O.J.S., Meiri, S., Donnellan, S.C., Richards, S.J., Austin, C.C., Oliver, P.M. 2019. The other side of the Sahulian coin: biogeography and evolution of Melanesian forest dragons. Biol. J. Linn. Soc. blz125. https://doi.org/10.1093/biolinnean/blz125.

Tallowin, O.J.S., Tamar, K., Meiri, S., Allison, A., Kraus, F., Richards, S.J., Oliver, P.M. 2018. Early insularity and subsequent mountain uplift were complementary drivers of diversification in a Melanesian lizard radiation (Gekkonidae: *Cyrtodactylus*). Mol. Phylogenet. Evol. 125, 29-39. https://doi.org/10.1016/j.ympev.2018.03.020.

Toussaint, E.F.A., Hall, R., Monaghan, M.T., Sagata, K., Ibalim, S., Shaverdo, H.V., Vogler, A.P., Pons, J., Balke, M. 2014. The towering orogeny of New Guinea as a trigger for arthropod megadiversity. Nat. Commun. 5, 4001. https://doi.org/10.1038/ncomms5001.

Uetz, P., Freed, P., Hošek, J. 2019. The Reptile Database. http://www.reptile-database.org (accessed 23 April 2019).

Vogt, T. 1932 Beitrag zur Reptilienfauna der ehemaligen Kolonie Deutsch-Neuguinea. Sitzungsber. Ges. naturf. Freunde Berlin. 1932, 281-294.

Weiler, P.D., Coe, R.S. 2000. Rotations in the actively colliding Finisterre Arc Terrane: paleomagnetic constraints on Plio-Pleistocene evolution of the South Bismarck

1013 microplate, northeastern Papua New Guinea. Tectonophysics. 316, 297-325.
1014 https://doi.org/10.1016/S0040-1951(99)00259-0.
1015 Weir, J.T. 2006. Divergent timing and patterns of species accumulation in lowland
1016 and highland neotropical birds. Evolution. 60, 842-855. https://doi.org/10.1111/j.0014-
1017 3820.2006.tb01161.x.
1018 Wiens, J.J., Graham, C.H. 2005. Niche conservatism: integrating evolution, ecology,
1019 and conservation biology. Annu. Rev. Ecol. Evol. Syst. 36, 519-539.
1020 https://doi.org/10.1146/annurev.ecolsys.36.102803.095431.
1021 Willig, M.R., Kaufman, D.M., Stevens, R.D. 2003. Latitudinal gradients of biodiversity:
1022 pattern, process, scale, and synthesis. Annu. Rev. Ecol. Evol. Syst. 34, 273-309.
1023 https://doi.org/10.1146/annurev.ecolsys.34.012103.144032.
1024 Yang, Z. 2015. The BPP program for species tree estimation and species delimitation.
1025 Curr. Zool. 61, 854-865. https://doi.org/10.1093/czoolo/61.5.854.
1026 Yang, Z., Rannala, B. 2010. Bayesian species delimitation using multilocus sequence
1027 data. Proc. Natl. Acad. Sci. USA. 107, 9264-9269.
1028 https://doi.org/10.1073/pnas.0913022107.
1029 Yang, Z., Rannala, B. 2014. Unguided species delimitation using DNA sequence data
1030 from multiple loci. Mol. Biol. Evol. 31, 3125-3135.
1031 https://doi.org/10.1093/molbev/msu279.
1032 Zhang, C., Zhang, D.-X., Zhu, T., Yang, Z. 2011. Evaluation of a Bayesian coalescent
1033 method of species delimitation. Syst. Biol. 60, 747-761.
1034 https://doi.org/10.1093/sysbio/syr071.
1035 Zweifel, R.G. 1980. Results of the Archbold expeditions. No. 103. Frogs and lizards
1036 from the Huon Peninsula, Papua New Guinea. Bull. Amer. Mus. Nat. Hist. 165, 387-434.